ORNL/TM-2002/293
NUREG/CR-XXXX

Fracture Toughness of an Irradiated, Highly Embrittled Reactor Pressure Vessel Weld

Manuscript Completed: October 2003
Date Submitted: December 2003
Date Published:

Prepared by
M. A. Sokolov, R. K. Nanstad, I. Remec, C. A. Baldwin, and R. L. Swain

Oak Ridge National Laboratory
Managed by UT-Battelle, LLC
Oak Ridge, TN 37831-6161

C. J. Fairbanks, NRC Project Manager

Prepared for
Division of Engineering Technology
Office of Nuclear Regulatory Research
U.S. Nuclear Regulatory Commission
Washington, DC 20555-0001
NRC Job Code W6953

Abstract

The Heavy-Section Steel Irradiation (HSSI) Program at Oak Ridge National Laboratory includes a task to investigate the shape of the fracture toughness master curve for reactor pressure vessel (RPV) steels that have become highly embrittled as a consequence of irradiation exposure. A radiation-sensitive RPV weld with intentionally enhanced copper content, designated KS-01, is characterized in terms of static initiation (K_{Ic}, K_{Jc}) and Charpy impact toughness in the unirradiated and irradiated conditions. The objectives of this project are to investigate the ability of highly embrittled material to maintain the shape of the unirradiated transition fracture toughness curve and to examine the ability of the Charpy 41-J shift to predict the fracture toughness shift at such high levels of embrittlement. Irradiation of this weld was performed at the University of Michigan Ford Nuclear Reactor in the new HSSI Irradiation-Anneal-Reirradiation facility. This reusable facility allows the irradiation of either virgin or previously irradiated material in a well-controlled temperature regime, including the ability to perform in situ annealing. Specimens of the KS-01 weld were irradiated to about 0.74×10^{19} neutrons/cm^2 at 288°C. Irradiation resulted in a Charpy ductile-to-brittle transition temperature shift of 169°C. It was anticipated that this shift would result in a fracture toughness transition temperature (at 100 MPa√m) in the irradiated condition near or slightly above the pressurized thermal shock screening criterion for circumferential welds, an RT_{PTS} of 300°F (149°C) according to the *Code of Federal Regulations*, Title 10, Part 50 (10 CFR 50). This was determined in terms of the master curve transition temperature T_{oPTS} = 129°C, using American Society of Mechanical Engineers Code Case N-629, which allows RT_{NDT} to be replaced by $RT_{To} = T_o + 35$°F (20°C). The fracture toughness characterization of the KS-01 weld in the unirradiated and irradiated conditions was mainly performed by testing 1T C(T) specimens, although some 0.5T C(T) and precracked Charpy specimens were also used in this study.

Foreword

The work reported here describes the Oak Ridge National Laboratory, Heavy-Section Steel Irradiation (HSSI) Program's investigation of the ability of highly embrittled material to maintain the shape of the unirradiated transition fracture-toughness curve, as well as to examine the ability of the Charpy 41-J shift to predict the fracture-toughness shift at such a high level of embrittlement. A radiation-sensitive reactor pressure vessel (RPV) weld with intentionally enhanced copper content, supplied by MPA Stuttgart and designated KS-01, is characterized, using the master curve methodology in terms of static initiation (K_{Ic}, K_{Jc}) and Charpy impact toughness in the unirradiated and irradiated conditions. Irradiation of this weld was performed at the University of Michigan Ford Nuclear Reactor in the HSSI Reusable Irradiation Facility.

The master curve methodology has become a widely accepted technique to characterize fracture toughness of RPV materials before and after irradiation. This methodology offers unique tools to describe the scatter of fracture toughness in the transition region, to account for size effects, and to provide one single parameter, the reference fracture toughness transition temperature, T_o, that characterizes the whole transition region.

Despite a high level of embrittlement and hardening, relationships between embrittlement and hardening of the KS-01 weld follow the general trend for RPV steels. This weld exhibited a low-ductile-initiation toughness (J_Q) after irradiation. It leaves a relatively narrow range of temperature within which to examine the shape of the transition region curve. Irradiated median fracture toughness values up to 148 MPa√m follow the master curve shape. However, low-toughness brittle fractures occurred at temperatures further above T_o than expected (T_o + 61°C), with a corresponding leveling of the crack initiation, K_{Jc}, values; i.e., the data did not follow the expected master curve shape.

This investigation is part of a larger effort to provide the Nuclear Regulatory Commission with a thorough and quantitative assessment of the effects of neutron irradiation on the material behavior and, in particular, the fracture toughness properties, of typical RPV steels as they relate to light-water RPV integrity. Results generated from these experiments will be incorporated into codes and standards that are used to resolve major regulatory issues related to RPV embrittlement, such as pressurized thermal shock, operating pressure-temperature limits, and low-temperature overpressurization. These issues are of particular importance as the nuclear power-plant industry applies for license extensions that will result in greater accumulated fluence over the lifetime of operation. As part of the HSSI Program, the work listed below has enabled the NRC to reduce the uncertainty in its regulatory process with respect to RPV embrittlement, thereby in part allowing the industry to consider license renewal.

Carl. J. Paperiello, Director

Office of Nuclear Regulatory Research

U.S. Nuclear Regulatory Commission

Contents

Abstract iii

Foreword v

Figures ix

Tables xi

Abbreviated Terms xiii

Acknowledgments xv

Introduction 1

Material Selection, Specimen Configurations, and Irradiation Conditions 3

Tensile Properties 9

Charpy Impact Properties 11

Fracture Toughness Properties 14

Summary and Conclusions 23

References 25

Appendix A. Neutronics Analysis of the First Two HSSI-IAR Metallurgical Capsules A-1

Appendix B. Publications List B-1

Figures

1. Distribution of surveillance specimen sets in the PR-EDB relative to their copper content and location of the KS-01 weld within this database 3

2. Distribution of surveillance specimen sets in the PR-EDB relative to their nickel content and location of the KS-01 weld within this database 4

3. Distribution of surveillance specimen sets in the PR-EDB relative to their manganese content and location of the KS-01 weld within this database 4

4. Distribution of surveillance specimen sets in the PR-EDB relative to their chromium content and location of the KS-01 weld within this database 5

5. X-ray compositional microanalysis results across the thickness of C(T) specimen 2-5 from the KS-01 weld 6

6. X-ray compositional microanalysis results across the thickness of C(T) specimen 3-1 from the KS 01 weld..... 6

7. X-ray compositional microanalysis results across the thickness of C(T) specimen 4-2 from the KS-01 weld 7

8. X-ray compositional microanalysis results across the thickness of C(T) specimen 8-42 from the KS-01 weld 7

9. Distribution of surveillance sets in the PR-EDB relative to their T_{41J} values and location of the KS-01 weld within the database 8

10. Embrittlement data of the KS-01 weld as provided by MPA-Stuttgart..... 9

11. Distribution of surveillance specimen sets in the PR-EDB relative to their yield strength and location of the KS-01 weld within this database 10

12. Yield strength and ultimate strength of the KS-01 weld before and after irradiation..... 11

13. Charpy impact energy vs test temperature for the KS-01 weld in the unirradiated condition (open symbols) and following irradiation (grey symbols) at 288°C to an average fast fluence of 0.74×10^{19} neutrons/cm^2 (E > 1 MeV)..... 13

14. Comparison of J-R curves developed from unirradiated and irradiated specimens 17

15. Relationship between absolute values of T_o and T_{41J} from Ref. [5] and the position of the KS-01 weld in the unirradiated and irradiated conditions..... 19

16. Relationship between fracture toughness T_o and Charpy T_{41J} shift for RPV steels from Ref. [5] and HSSI data only from Ref. [8] and position of the KS-01 weld from the present study 20

17. Relationship between fracture toughness T_o shift and yield strength increase for RPV steels from Ref. [5] and position of the KS-01 weld from the present study 20

18. 1T size-adjusted fracture toughness data of the KS-01 weld before and after irradiation 21

19. Median fracture toughness values of the KS-01 weld in the unirradiated and irradiated conditions relative to their master curves 21

A.1 Horizontal cross section of the HSSI/UCSB irradiation facility at FNR A-5

A.2 Metallurgical specimens and neutron dosimeters loaded in capsule 1, which started irradiation in the north location in the HSSI-IAR facility A-6

A.3 Metallurgical specimens and neutron dosimeters loaded in capsule 2, which started irradiation in the south location in the HSSI-IAR facility A-7

Tables

1. Chemical composition of the KS-01 weld 3

2. Average values and standard deviations of X-ray microanalysis measurements of compact specimens of the KS-01 weld 6

3. Tensile properties of the KS-01 weld in the unirradiated condition 10

4. Tensile properties of the KS-01 weld specimens tested after irradiation at 288°C to 0.76×10^{19} neutrons/cm^2 11

5. Charpy impact data of the KS-01 weld in the unirradiated condition as measured by MPA and ORNL 12

6. Charpy impact data of the KS-01 weld after irradiation at 288°C to 0.74×10^{19} neutrons/cm^2 (E > 1 MeV) 13

7. Summary of Charpy impact properties of the KS-01 weld material before and after irradiation 14

8. Fracture toughness values of unirradiated KS-01 weld measured in the transition region 16

9. MPA fracture toughness measurements of the KS-01 weld 17

10. Median fracture toughness values of unirradiated KS-01 weld 17

11. Fracture toughness data of the KS-01 weld after irradiation at 288°C to 0.74×10^{19} neutrons/cm^2 (E > 1 MeV) 18

12. Median fracture toughness values (adjusted to 1T) for irradiated KS-01 weld 21

A.1 Measured specific activities of the dosimeters in Capsule 1 ..... A-8

A.2 Measured specific activities of the dosimeters in Capsule 2 ..... A-10

A.3 Measured specific activities of the dosimeters from the HSSI-IAR RDTs 07 (North) and 08 (South) A-11

A.4 Measured specific activities of the dosimeters from the HSSI-IAR RDTs 09 (North) and 10 (South) A-12

A.5 Irradiation history for the HSS-IAR1 capsule (which started in north position) and HSS-IAR2 capsule A-13

A.6 Calculated and adjusted fast-neutron fluence (E > 1 MeV) for the dosimeters located in capsule 1 ..... A-15

A.7 Calculated and adjusted fast-neutron fluence (E > 1 MeV) for the dosimeters located in capsule 2 ..... A-17

A.8 Adjusted irradiation parameters at the locations of the dosimeters in capsule 1 ..... A-18

A.9 Adjusted irradiation parameters at the locations of the dosimeters in capsule 2 ..... A-19

Abbreviated Terms

Nomenclature

σ_{US}	ultimate strength
σ_{YS}	yield strength
0.5T (CT)	compact tension specimen with thickness of 0.5 in.
1T (CT)	compact tension specimen with thickness of 1 in.
J_c	the J-integral at the point of onset of cleavage fracture
J_Q	ductile initiation toughness
K_{Jc}	an elastic-plastic equivalent stress intensity factor derived from J_c
RT_{NDT}	reference nil-ductility temperature
RT_{PTS}	pressurized thermal shock screening criteria
T_{41J}	Charpy transition temperature at absorbed energy = 41 J
T_{68J}	Charpy transition temperature at absorbed energy = 68 J
T_o	reference fracture toughness temperature at $K_{Jc(med)}$ = 100 MPa√m

Acronyms and Abbreviations

ASME	American Society of Mechanical Engineers
ASTM	American Society of Standards and Materials
CVN	Charpy V-notch
DBTT	ductile-to-brittle transition temperature
EOI	end of irradiation
FRD	fission radiometric dosimetry set
HSSI	Heavy Section Steel Irradiation
IAR	Irradiation Anneal Reirradiation
LVDT	linear variable differential transformer
PCVN	precracked Charpy V-notch
PR-EDB	Power Reactor Embrittlement Database
RDT	removable dosimetry tube
RPV	reactor pressure vessel
UCSB	University of California at Santa Barbara
USE	upper-shelf energy

Acknowledgments

The work reported here was performed at the Oak Ridge National Laboratory (ORNL) under the Heavy-Section Steel Irradiation (HSSI) Program, T. M. Rosseel, Program Manager. The HSSI Program is sponsored by the Office of Nuclear Regulatory Research, U.S. Nuclear Regulatory Commission (NRC), under Interagency Agreement DOE 1886-N695-3W with the U.S. Department of Energy, under Contract No. DE-AC05-00OR22725 with UT-Battelle, LLC. The technical monitor for the NRC is C. J. Fairbanks. That support is gratefully acknowledged.

The authors would also like to thank Drs. E. Roos, J. Fohl, and U. Eisele, of MPA Stuttgart and Dr. R. Langer, Framatome-Siemens, for providing the KS01 weld metal and for sharing their experience and knowledge of this weld.

Introduction

The master curve methodology has become a widely accepted technique to characterize fracture toughness of reactor pressure vessel (RPV) materials before and after irradiation. This methodology offers unique tools to describe the scatter of fracture toughness in the transition region, to account for size effects, and to provide one single parameter, the reference fracture toughness transition temperature, T_o, to characterize the whole transition region. All of these factors have made this methodology well accepted for RPV steels, and it is used now for some other ferritic steels as well, although experience with the latter materials is limited as compared to that with RPV steels.

The shape of the master curve was established with unirradiated and some irradiated fracture toughness data [1] as an empirical fit to these data, size adjusted to 1T. Most of the fracture toughness data support this empirical approximation; however, the physical basis for the universal shape of the transition fracture toughness curve remains open for discussion. That uncertainty raises concerns regarding the ability of a highly embrittled material to maintain the same shape of the transition fracture toughness curve as it would in the unirradiated condition and necessitates the experimental validation of this assumption. Such concerns are based on several considerations. One consideration is analogous to Charpy impact properties. It is well known that irradiation results in two main changes—a decrease in the upper-shelf energy (USE) and an increase (shift) in the ductile-to-brittle transition temperature (DBTT). It needs to be pointed out for purposes of this study that these changes are accompanied by an alteration in the shape of the Charpy impact transition curve. Since irradiation reduces the stable crack growth initiation toughness (J_{Ic}) and shifts the transition fracture toughness curve up in temperature, the concerns regarding the shape of the fracture toughness transition curve need to be addressed. In addition to the analogy to Charpy transition behavior, some limited irradiated fracture toughness data [2–5] also suggest a potential change in the shape of the fracture toughness transition curve as result of irradiation.

Experimental

Material Selection, Specimen Configurations, and Irradiation Conditions

The purpose of this pilot study was to perform fracture toughness characterization tests of a metallurgically modified RPV steel irradiated to a low fluence but with a level of embrittlement that would correspond to or slightly exceed the currently accepted end-of-life condition. The pressurized thermal shock screening criteria for weld metals, RT_{PTS}, are prescribed in the *Code of Federal Regulations*, Title 10, Part 50 (10 CFR 50) [6]. The criterion for circumferential welds is 300°F (149°C). This criterion was converted, in terms of the master curve transition temperature, to T_{oPTS} = 130°C, using American Society of Mechanical Engineers (ASME) Code Case N-629, which allows RT_{NDT} to be replaced by $RT_{To} = T_o$ + 35°F (19°C).

After several options were considered, an offer of material from MPA-Stuttgart in Germany was accepted, based on the requirement that the material achieve a high embrittlement level after a relatively short test reactor irradiation. The weld, designated KS-01, has intentionally increased copper, nickel, and manganese contents (as can be seen in Table 1). Chromium content is also high relative to a typical U.S.-made RPV weld, but it is more common for German-made welds. The contents of copper, nickel, manganese, and chromium in the KS-01 weld are shown in Figs. 1 through 4 relative to the data extracted by R. E. Stoller from the RPV surveillance Power Reactor Embrittlement Database (PR-EDB) [7].

Table 1. Chemical composition of the KS-01 weld

C	Ni	Mn	Mo	Cr	Cu	Si	P	S
0.06	1.23	1.64	0.70	0.47	0.37	0.18	0.017	0.012

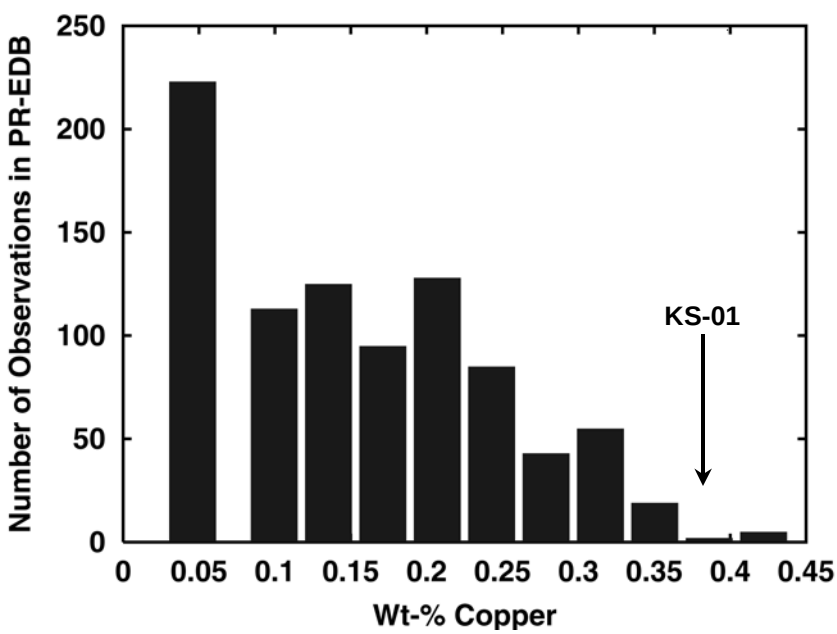

Fig. 1. Distribution of surveillance specimen sets in the PR-EDB relative to their copper content and location of the KS-01 weld within this database.

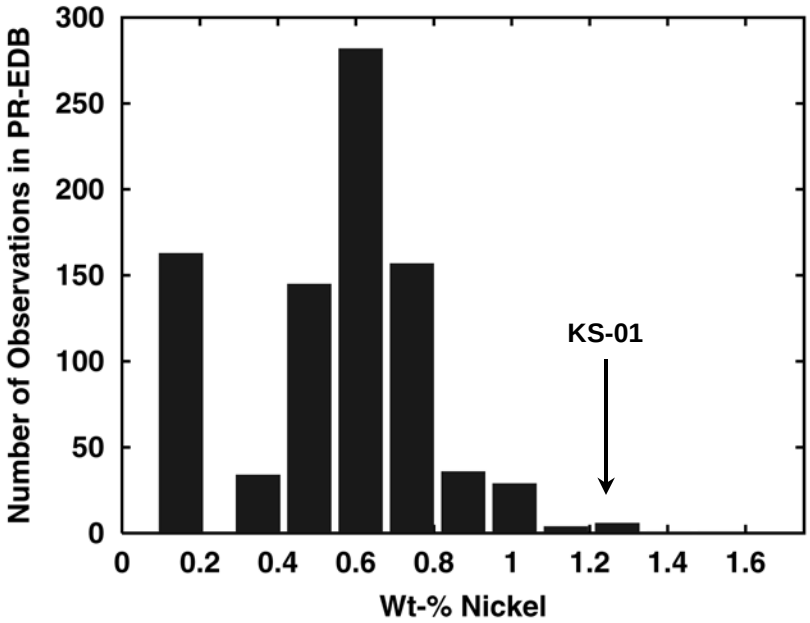

Fig. 2. Distribution of surveillance specimen sets in the PR-EDB relative to their nickel content and location of the KS-01 weld within this database.

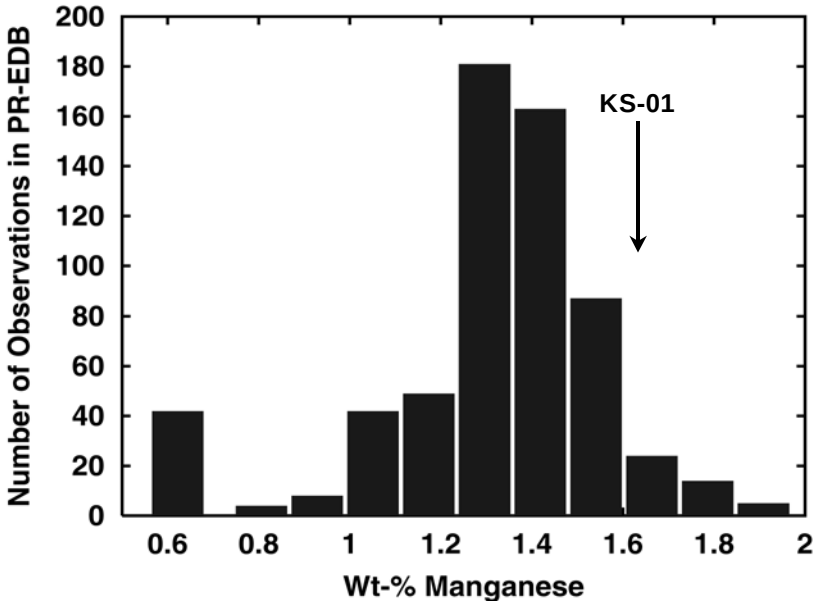

Fig. 3. Distribution of surveillance specimen sets in the PR-EDB relative to their manganese content and location of the KS-01 weld within this database.

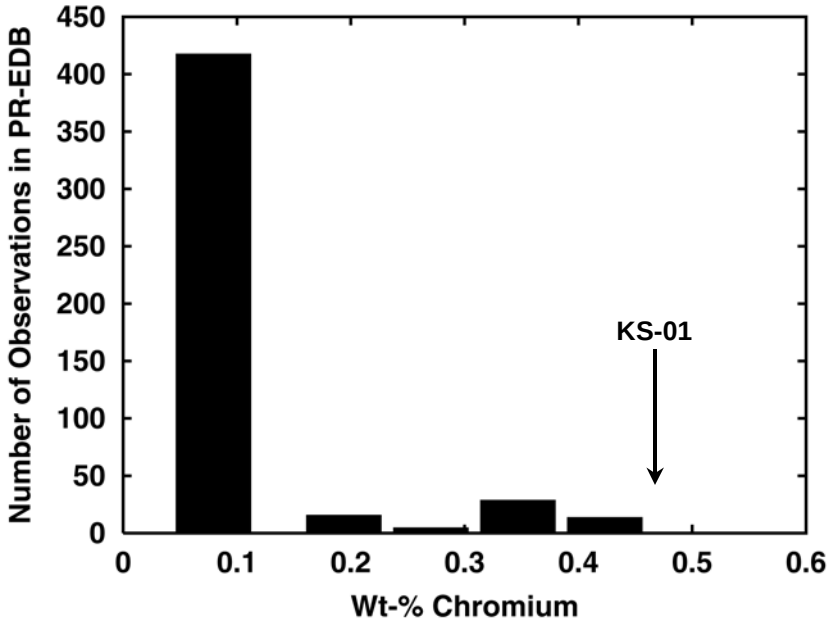

Fig. 4. Distribution of surveillance specimen sets in the PR-EDB relative to their chromium content and location of the KS-01 weld within this database.

The KS-01 weld was used in a German irradiation research program, and it exhibited extremely high sensitivity to radiation. MPA provided the weld together with mechanical properties in the unirradiated and irradiated conditions. Most of the data provided were Charpy impact and tensile properties before and after irradiation, although a limited amount of fracture toughness (linear-elastic K_{Ic}) data was also provided. Since basic properties in the unirradiated condition were available, it was decided to dedicate most of the material to irradiation testing and to perform only limited tests in the unirradiated condition to confirm the MPA data. Based on the amount of weld provided, it was decided to perform irradiation of 21 1T C(T), 12 0.5T C(T), 21 precracked Charpy, 22 standard Charpy V-notch (CVN), and 8 tensile specimens. Additionally, a few subsize, precracked Charpy specimens and coupons for atom-probe and small-angle neutron scattering characterization were included for irradiation. Only the 0.5T C(T) specimens were 20% side-grooved. The other specimens were irradiated and tested without side grooves.

The weld material was provided in several blocks. 1T C(T) specimens were machined from four different blocks. One of the tested compact specimens from each block was polished for X-ray microcompositional analysis. X-ray microcompositional analyses were conducted to examine elemental variations across the thickness of specimens. Fifteen measurements were made across the thickness of each specimen. Average values for the chemical composition of each specimen are given in Table 2, and Figs. 5 through 8 provide results of X-ray spectroscopy scans across each specimen. The mean values are in good agreement with the bulk analyses given in Table 1, except for manganese content. X-ray microanalysis consistently provided higher values than the MPA data.

Table 2. Average values and standard deviations of X-ray microanalysis measurements of compact specimens of the KS-01 weld

Specimen ID	Element, wt % ± 1σ					
	Mn	Cr	Ni	Si	Mo	Cu
2-5	1.88±0.11	0.49±0.01	1.19±0.10	0.18±0.02	0.69±0.04	0.34±0.01
3-1	1.97±0.13	0.48±0.01	1.19±0.08	0.21±0.03	0.68±0.03	0.37±0.02
4-2	1.98±0.11	0.48±0.01	1.21±0.08	0.19±0.03	0.67±0.02	0.36±0.02
8-42	1.94±0.08	0.49±0.02	1.17±0.12	0.17±0.02	0.67±0.03	0.34±0.02

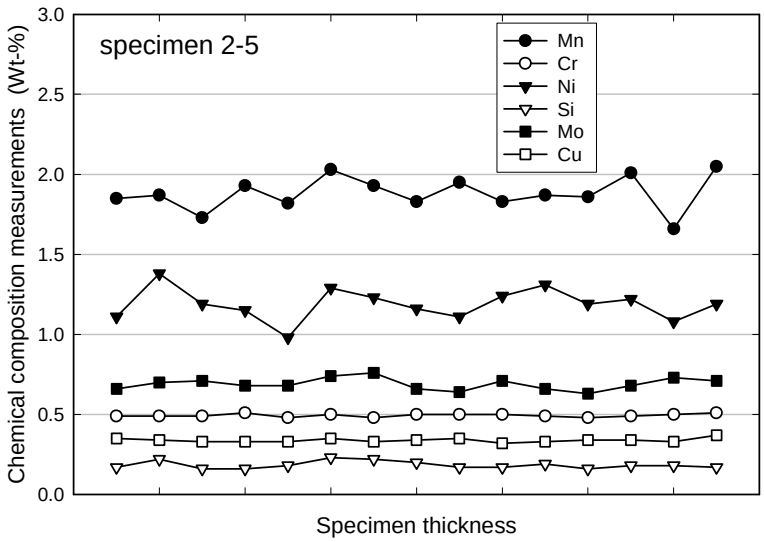

Fig. 5. X-ray compositional microanalysis results across the thickness of C(T) specimen 2-5 from the KS-01 weld.

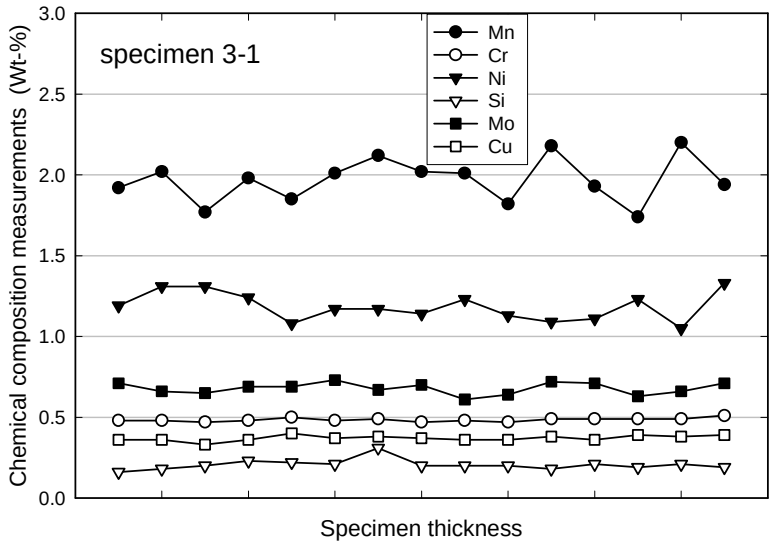

Fig. 6. X-ray compositional microanalysis results across the thickness of C(T) specimen 3-1 from the KS-01 weld.

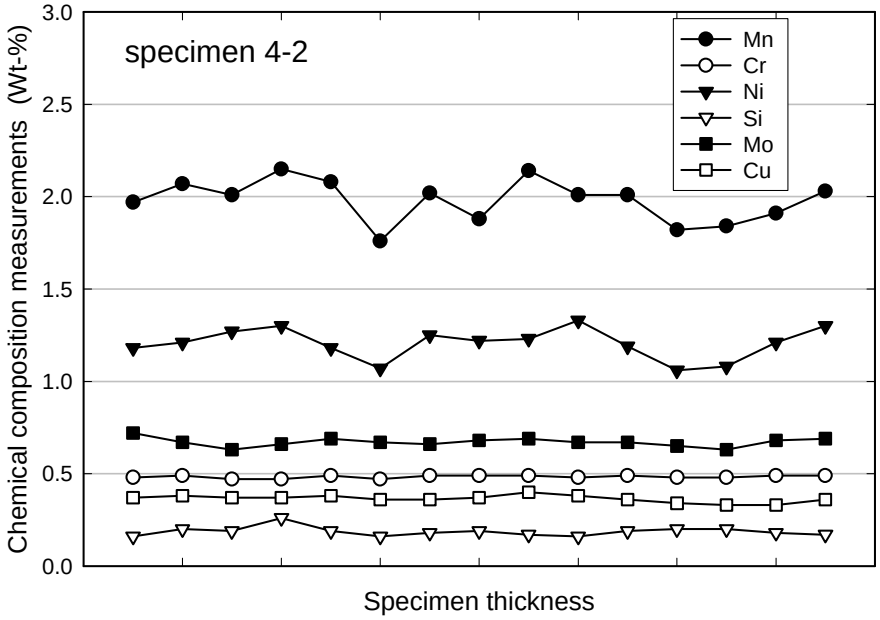

Fig. 7. X-ray compositional microanalysis results across the thickness of C(T) specimen 4-2 from the KS-01 weld.

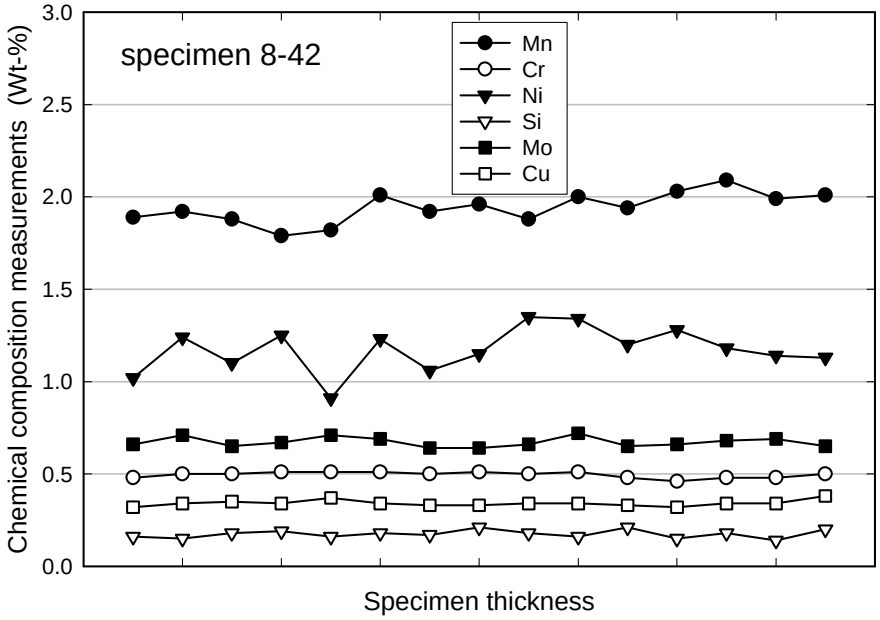

Fig. 8. X-ray compositional microanalysis results across the thickness of C(T) specimen 8-42 from the KS-01 weld.

The Charpy DBTT, T_{41J}, in the unirradiated condition was −10°C according to the MPA data. For comparison purposes, Fig. 9 represents the unirradiated T_{41J} temperature of the KS-01 weld relative to those within the PR-EDB. By using the MPA data and the following correlation between T_o and T_{41J} from Ref. [8],

$$T_o = T_{41J} - 24°C, \tag{1}$$

it was anticipated that the reference fracture toughness temperature, T_o, of the KS-01 weld in the unirradiated condition would be about −34°C. The purpose of this pilot study was to perform fracture toughness characterization tests of a material with a value of T_o in the irradiated condition that would be equal to or slightly exceed T_{oPTS} = 130°C. Thus, a target fluence was selected that would induce a Charpy DBTT shift of about 170°C. Based on the MPA data, the neutron fluence of about 0.8×10^{19} neutrons/cm^2 (E > 1 MeV) was selected as the target fluence for this irradiation experiment (see Fig. 10). It was also anticipated that irradiation to this fluence would not decrease the Charpy USE below 68 J (50 ft-lb), in accordance with the requirements of 10 CFR 50, Appendix G.

Irradiation was performed in the Heavy Section Steel Irradiation Irradiation-Anneal-Reirradiation (HSSI-IAR) facility at the University of Michigan Ford Nuclear Reactor, in reusable capsules, at 288°C. Details of capsule layout, irradiation history, and neutronics analyses of the specimens are given in the appendix to this document. In general, the capsules consist of five cells each. The capsules were designed in such a way that each cell would accommodate three 1T C(T) specimens or their equivalent. The entire facility with capsules can be retrieved from the reactor at any time, which allows complete control of the desired fluence during irradiation. Additionally, capsules can be removed from the facility and moved into a hot cell, and the capsule covers can be opened or closed remotely while in the hot cell for changing or replacing specimens.

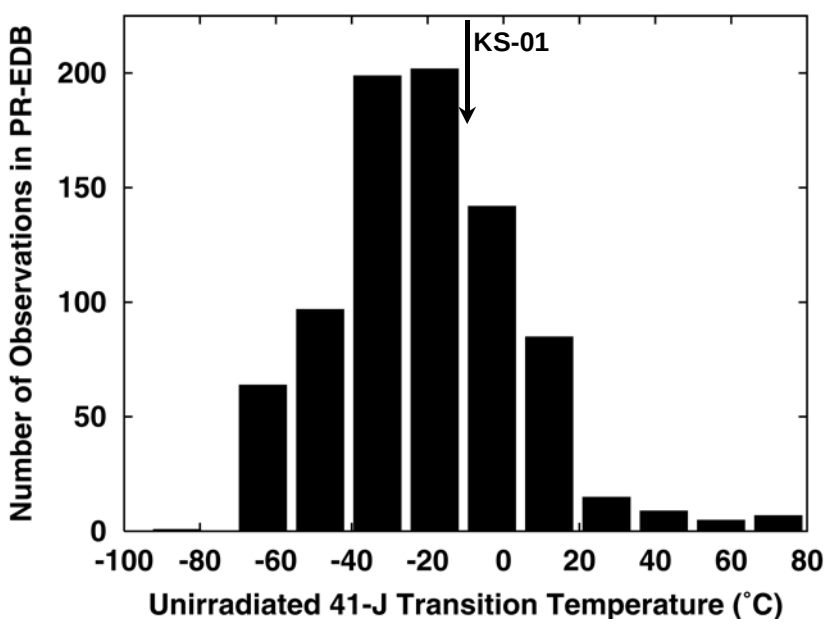

Fig. 9. Distribution of surveillance sets in the PR-EDB relative to their T_{41J} values and location of the KS-01 weld within the database.

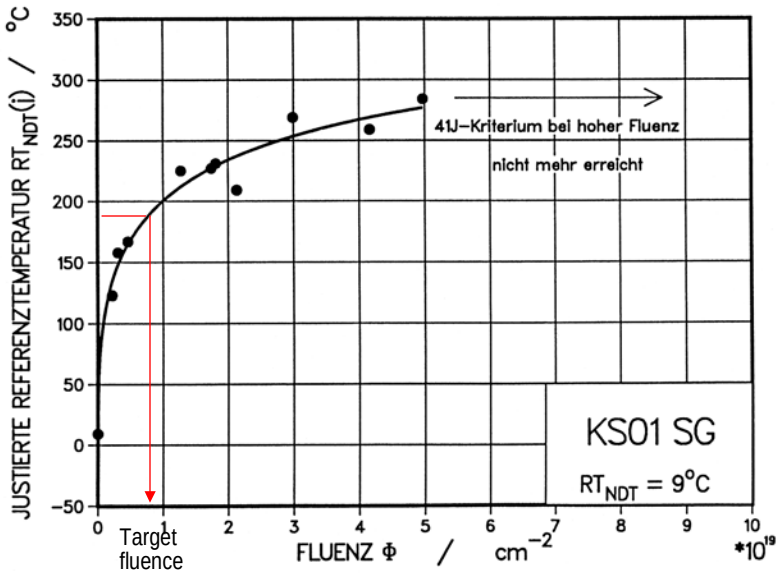

Fig. 10. Embrittlement data of the KS-01 weld as provided by MPA-Stuttgart.

Multizone electrical heaters installed in the facility maintain the temperature within the capsules to ± 2°C. The combination of these factors makes this HSSI-IAR facility a unique instrument to perform well-controlled irradiation experiments with RPV steels. See Ref. [9] for a detailed description of the facilities.

At the midpoint of the irradiation process, capsules with KS-01 specimens were retrieved from the reactor and opened, and specimens were repositioned within the capsule in order to smooth the flux distribution among the specimens. Capsules were also rotated 180° to average the neutron flux through the capsule thickness.

Most of the specimens were exposed to a neutron dose that varied from 0.70 to 0.84 × 10^{19} neutrons/cm^2 (E > 1 MeV). However, there was one cell containing three 1T C(T) specimens for which the fluence only varied from 0.62 to 0.64 × 10^{19} neutrons/cm^2 (E > 1 MeV). Tables in this report contain information about the total accumulated fluence for each specimen.

Tensile Properties

Testing of round tensile specimens with a gage section of 5.08 mm in diameter and 31.75 mm in length was conducted in accordance with American Society for Testing and Materials (ASTM) standard E-8 [10]. Four tensile specimens were tested in the unirradiated condition. Two specimens were tested at room temperature, and two at −60°C. These two temperatures were selected to cover the temperature range in which fracture toughness specimens could be tested and also because MPA data were available at those temperatures. Overall, MPA tested unirradiated tensile specimens in the temperature range from –100°C to 275°C. Table 3 summarizes yield strength (σ_{YS}) and ultimate strength (σ_{US}) data obtained at both ORNL and MPA on the unirradiated KS-01 weld.

Table 3. Tensile properties of the KS-01 weld in the unirradiated condition

Test temperature, °C	Laboratory	Yield strength, MPa	Ultimate strength, MPa
−100	MPA	694	794
−60	MPA	644	744
−60	ORNL	661	761
−60	ORNL	645	752
−20	MPA	619	709
23	MPA	599	679
23	ORNL	598	680
23	ORNL	603	689
80	MPA	582	654
140	MPA	564	634
200	MPA	544	619
275	MPA	519	602

Tensile properties of the KS-01 weld measured at ORNL and MPA are in very good agreement. On average, room temperature yield strength is 600 MPa and ultimate strength is 683 MPa in the unirradiated condition. This material has a relatively high strength in the unirradiated condition compared with that of a typical RPV weld (see Fig. 11). This was initially considered an advantage because high yield strength increases the validity limit for fracture toughness measurements according to ASTM standard E 1921-02 [11]. After irradiation, seven specimens were tested in the temperature range from –100°C to 250°C (see Table 4). The yield strength at room temperature increased by 226 MPa, and ultimate strength increased by 203 MPa, compared with results for specimens tested in the unirradiated condition. The average fluence among tensile specimens was 0.762×10^{19} neutrons/cm^2 (E > 1 MeV) with a standard deviation of 0.018×10^{19} neutrons/cm^2.

Figure 12 summarizes the temperature dependencies of yield and ultimate strengths of the KS-01 weld in both the unirradiated and irradiated conditions.

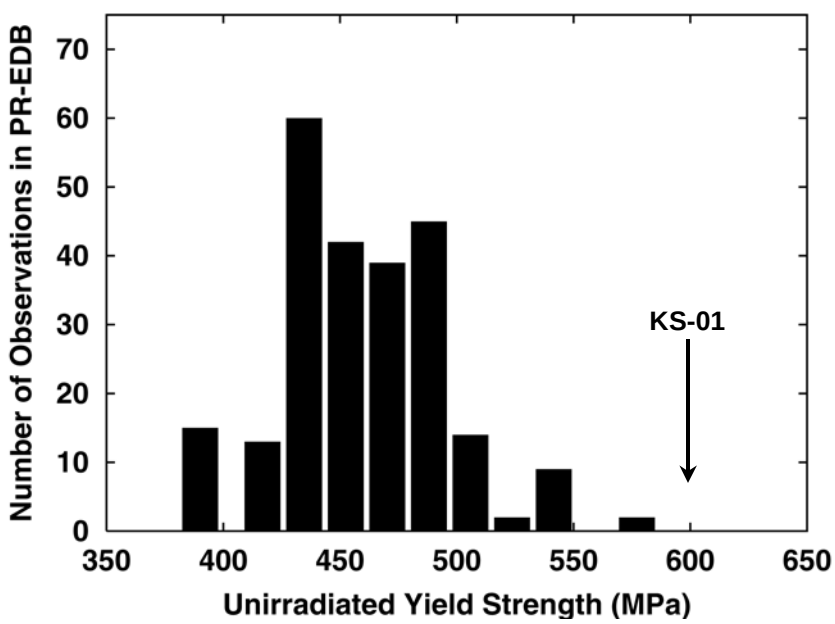

Fig. 11. Distribution of surveillance specimen sets in the PR-EDB relative to their yield strength and location of the KS-01 weld within this database.

Table 4. Tensile properties of KS-01 weld specimens tested after irradiation at 288°C to 0.76×10^{19} neutrons/cm^2

Specimen ID	T8-33	T8-12	T8-11	T8-13	T8-23	T8-39	T8-24
Neutron fluence, 10^{19} n/cm^2	0.76	0.775	0.739	0.739	0.76	0.787	0.775
Test temperature, °C	−100	24	24	100	150	200	250
Yield strength, MPa	890	828	825	779	756	746	743
Ultimate strength, MPa	965	885	889	844	820	809	802

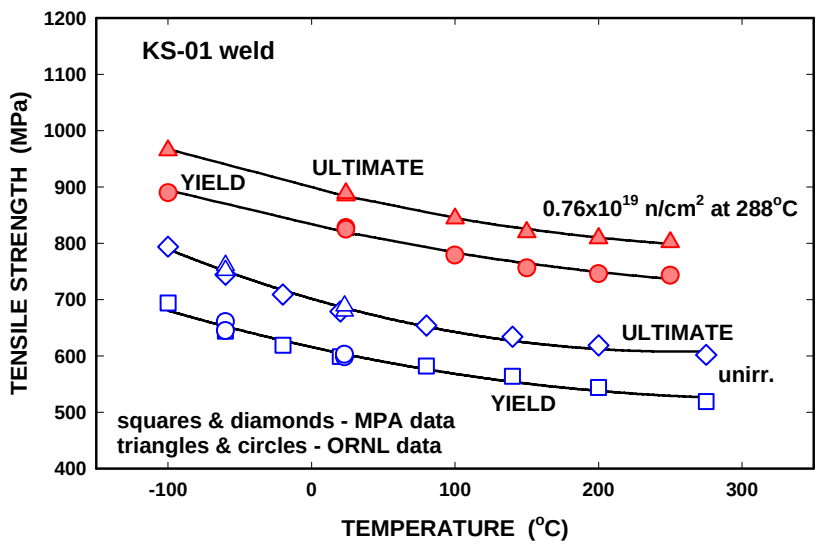

Fig. 12. Yield strength and ultimate strength of the KS-01 weld before and after irradiation.

Charpy Impact Properties

Testing of CVN specimens was conducted in accordance with ASTM standards E23 and E185 [12,13]. Specimens were oriented in the transverse-longitudinal (TL) orientation. Fifteen CVN specimens were tested in the unirradiated condition by MPA, and ten specimens were tested by ORNL. The results are given in Table 5. As in the case with tensile properties, CVN data from both laboratories are in very good agreement. The Charpy transition temperature, T_{41J}, is –10°C, and the USE is 118 J.

Twenty-two specimens were tested after irradiation at 288°C to 0.74×10^{19} neutrons/cm^2 (E > 1 MeV); the results are given in Table 6. As expected, the KS-01 weld exhibited a large shift of transition temperature, 169°C. The USE was reduced to 78 J. Figure 13 presents the Charpy impact properties of KS-01 weld material before and after irradiation. In addition to a large shift of transition temperature and drop in the USE, this weld also exhibited a change in the slope of the transition region curve typical for irradiated RPV materials. For example, the shift of T_{41J} was 169°C compared with the 217°C shift of T_{68J}. The combination of these factors has made the KS-01 weld a perfect candidate for purposes of this study.

Table 7 provides a summary of Charpy impact properties of KS-01 weld material before and after irradiation. The Charpy impact parameters were determined from curve fits using a hyperbolic tangent function with lower shelves fixed to 2.7 J for energy, 0.0 mm for lateral expansion, and 0% for shear appearance. The average neutron fluence among Charpy specimens was 0.742×10^{19} neutrons/cm^2 with a standard deviation of 0.018×10^{19} neutrons/cm^2 (E > 1 MeV).

Table 5. Charpy impact data of the KS-01 weld in the unirradiated condition as measured by MPA and ORNL

Specimen ID	Temperature, °C	Energy, J	Lateral expansion, mm	Shear, %
		ORNL		
6-14	−75	2.03	0.15	0
6-1	−50	9.49	0.20	20
6-2	−25	31.86	0.58	50
6-3	0.0	56.27	0.84	60
6-7	25	68.47	1.40	85
6-8	50	92.87	1.52	100
6-17	75	98.3	1.65	100
6-5	100	107.79	1.78	100
6-4	200	117.28	1.91	100
6-6	275	123.38	2.08	100
		MPA		
XN75	−80	7.0	0.05	11
XN74	−65	10.0	0.08	16
XN45	−50	20.0	0.24	1
XN60	−35	13.0	0.15	19
XN44	−25	26.0	0.35	10
XN30	0.0	58.0	1.03	63
XNBP01	25	72.0	1.06	84
BN97	50	100.0	1.52	91
BN98	75	92.0	1.46	93
XN89	90	126.0	1.99	100
BN99	100	88.0	1.62	89
XN90	130	119.0	1.90	100
XN14	150	113.0	1.80	100
XN15	200	126.0	2.09	100
XN29	275	124.0	1.89	100

Table 6. Charpy impact data of the KS-01 weld after irradiation at 288°C to 0.74×10^{19} neutrons/cm^2 (E > 1 MeV)

Specimen ID	Neutron fluence, 10^{19} n/cm^2 (E > 1 MeV)	Temperature, °C	Energy, J	Shear, %
5-10	0.715	23	6.91	5
5-11	0.721	23	6.24	5
5-15	0.746	50	9.08	0
5-8	0.721	50	5.15	0
5-9	0.723	75	16.54	15
5-13	0.725	75	13.02	10
5-7	0.715	100	27.52	30
5-16	0.764	100	28.20	30
5-17	0.764	125	17.22	10
5-6	0.751	125	30.23	30
5-3	0.751	150	36.20	40
5-19	0.739	150	23.32	20
5-20	0.739	175	39.32	40
5-1	0.746	175	54.37	60
5-2	0.745	200	46.23	60
5-18	0.777	200	66.71	90
6-19	0.760	225	66.71	95
5-4	0.746	225	77.01	95
5-5	0.745	250	70.23	95
6-20	0.760	250	72.67	95
5-12	0.723	275	72.40	99
5-14	0.746	275	81.48	100

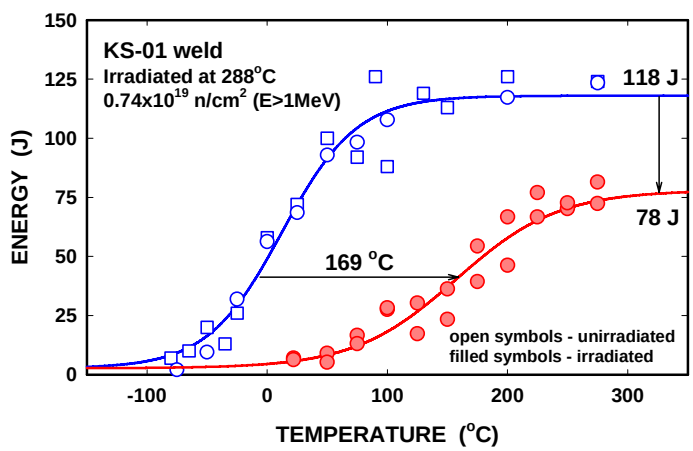

Fig. 13. Charpy impact energy vs test temperature for the KS-01 weld in the unirradiated condition (open symbols) and following irradiation (grey symbols) at 288°C to an average fast fluence of 0.74×10^{19} neutrons/cm^2 (E > 1 MeV).

Table 7. Summary of Charpy impact properties of the KS-01 weld material before and after irradiation

Charpy impact property	Before irradiation	After irradiation
T_{41J}, °C	−10	159
T_{68J}, °C	20	237
$T_{0.9mm}$, °C	6	Not measured
$T_{50\%}$, °C	−10	166
Upper shelf energy, J	118	78
Upper shelf lateral expansion, mm	1.92	Not measured

Fracture Toughness Properties

Fracture toughness data have been generated using compact specimens, C(T), of 0.5T and 1T sizes, although a limited number of precracked CVN (PCVN) specimens have been also tested in the unirradiated condition. Specimens were fabricated, precracked, and tested according to ASTM E 1921-02 [11]. Only the 0.5T C(T) specimens were 20% side-grooved (10% from each side) after fatigue precracking. An outboard clip gage was used to measure load-line displacement on the C(T) specimens, and a linear variable differential transformer (LVDT) gage was used to measure load-line displacement on the PCVN specimens. The unloading compliance method was used to obtain J-integral versus crack extension data. From J-integral versus crack extension data, a J-integral at the point of cleavage instability, J_c, was determined, and a critical value of the stress intensity factor, K_{Jc}, was calculated from

$$K_{Jc} = \sqrt{J_c \frac{E}{1-\nu^2}} \quad , \tag{2}$$

where E is Young's modulus and ν = 0.3 is Poisson's ratio. In the present work, the following fit to ASME data was used for the temperature dependence of Young's modulus:

$$E = 192520 - 66 \cdot T \ , \ \text{in MPa}, \tag{3}$$

where T is in °C.

It was decided to perform replicate fracture toughness tests at several test temperatures within the transition range, in both unirradiated and irradiated conditions. All K_{Jc} data were converted to 1T equivalence, $K_{Jc(1T)}$, using the size adjustment procedure of ASTM E 1921−02 [1,11]

$$K_{Jc(1T)} = 20 + \left[K_{Jc(x)} - 20\right] \cdot \left(\frac{B_x}{B_{1T}}\right)^{1/4} , \tag{4}$$

where $K_{Jc(x)}$ = measured K_{Jc} value,
B_x = gross thickness of test specimen,
B_{1T} = gross thickness of 1T C(T) specimen.

Attempts were made to test at least six specimens at a given temperature. That would allow determining the median fracture toughness as follows [11]:

$$K_{Jc(med)} = 20 + \left[\ln(2) \cdot \sum_{i=l}^{N} \frac{\left(K_{Jc(i)} - 20\right)^4}{r}\right]^{1/4} . \tag{5}$$

where

$K_{Jc(i)}$= either a valid K_{Jc} datum or a dummy substitute for an invalid datum (see definition of invalid data below),

r = number of valid data,

N = number of data (valid and invalid).

Two validity criteria were used to qualify K_{Jc} data. A K_{Jc} datum would be considered invalid if this value exceeded the $K_{Jc(limit)}$ requirement of E 1921−02 [11]:

$$K_{Jc(limit)} = \sqrt{\frac{b_o\,\sigma_{YS}}{30} \cdot \frac{E}{1-\nu^2}}\,, \tag{6}$$

where b_o is the in-plane size of the specimen's remaining ligament. As mentioned earlier, the KS-01 weld had a relatively high yield strength, even in the unirradiated condition, and irradiation increased it significantly. As a result, none of the specimens tested within this study violated the ligament-size validity requirement. The second validity requirement limits the amount of stable crack growth prior to cleavage instability. A K_{Jc} datum was considered invalid if the test terminated in cleavage after slow-stable crack growth of more than 0.05(W-a_o), or 1 mm, whichever is smaller. Several specimens in this study violated this requirement, and those K_{Jc} values were replaced by the highest valid K_{Jc} value in the data set for any given specimen size.

The reference fracture toughness transition temperature, T_o, was determined using the multi-temperature equation from ASTM E 1921−02 [1,11]:

$$\sum_{i=1}^{N} \delta_i \frac{\exp\left[0.019\left(T_i - T_o\right)\right]}{11+77\exp\left[0.019\left(T_i - T_o\right)\right]} - \sum_{i=1}^{N} \frac{\left(K_{Jc(i)} - 20\right)^4 \exp\left[0.019\left(T_i - T_o\right)\right]}{\left\{11+77\exp\left[0.019\left(T_i - T_o\right)\right]\right\}^5} = 0\,, \tag{7}$$

where

δ_i = 1.0 if the datum is valid, zero if the datum is a dummy substitute value,

T_i = test temperature corresponding to $K_{Jc(i)}$.

The K_{Jc} test data for the KS-01 weld in the unirradiated condition are presented in Table 8. In the same table, 1T equivalence data are also presented. Two of the specimens tested at room temperature cleaved after more than 1 mm of stable crack growth, and the data from these specimens were used as invalid data points for T_o and $K_{Jc(med)}$ determinations. One of the PCVN specimens, namely 8-72, cleaved with a K_{Jc} value just slightly lower than the $K_{Jc(limit)}$ for this specimen size/temperature (152.3 MPa√m).

In addition to transition region testing, two 0.5T C(T) specimens were tested to develop full J-R curves, one at 80°C and another at 120°C. Those J-R curves were analyzed according to ASTM standard E 1820 [14] and the critical J-integral values at onset of stable crack growth, J_{Ic}, were determined as 162.6 kJ/m^2 and 147 kJ/m^2, respectively.

MPA also performed fracture toughness characterization testing of KS-01 weld material in the unirradiated condition by using 1T and 2T C(T) specimens. These tests were limited to developing only linear-elastic K_{Ic} data in accordance with ASTM standard E 399 [15]. Nevertheless, these data were also used to evaluate the T_o value of KS-01 weld material in the unirradiated condition. MPA results are given in Table 9.

All data in Tables 8 and 9 were combined to determine an initial value of the transition temperature, T_o, using Eq. (7). After that, in accordance with ASTM E 1921-02, analysis was limited only to the data that were distributed over a restricted temperature range, namely $T_o \pm 50°C$. As a result, fracture toughness data developed at temperatures of –80°C and lower were excluded from the final analysis. The final value of the reference fracture toughness transition temperature for the KS-01 weld in the unirradiated condition is –26°C.

Table 10 presents median fracture toughness values of unirradiated KS-01 weld material at four test temperatures determined by using Eq. (5). The median fracture toughness value at –50°C was determined with six PCVN specimens and one 2T C(T) XB88 specimen.

Table 8. Fracture toughness values of unirradiated KS-01 weld measured in the transition region

Type of specimen	Specimen ID	J_c, kJ/m^2	K_{Jc}, Mpa√m	$K_{Jc(1T)}$, Mpa√m	Remarks
Test temperature −50°C					
PCVN	8-74	33.31	84.70	71.46	Valid
PCVN	8-73	26.6	75.69	64.29	Valid
PCVN	8-72	106.69	151.59	124.65	Valid
PCVN	8-71	28.53	78.39	66.44	Valid
PCVN	8-64	89.82	139.09	114.71	Valid
PCVN	8-63	31.81	82.77	69.92	Valid
Test temperature −35°C					
1T C(T)	4-4	31.72	82.44	82.44	Valid
1T C(T)	8-71	15.83	58.24	58.24	Valid
1T C(T)	8-73	13.93	54.64	54.64	Valid
1T C(T)	8-72	25.21	73.50	73.50	Valid
1T C(T)	4-2	26.56	75.44	75.44	Valid
1T C(T)	2-5	20.7	66.60	66.60	Valid
1T C(T)	8-42	26.55	75.43	75.43	Valid
1T C(T)	0-6	16.28	59.06	59.06	Valid
Test temperature −5°C					
1T C(T)	0-1	55.02	108.02	108.02	Valid
1T C(T)	0-2	53.73	106.75	106.75	Valid
1T C(T)	0-3	48.1	101.00	101.00	Valid
1T C(T)	0-4	48.62	101.55	101.55	Valid
1T C(T)	0-5	49.33	102.29	102.29	Valid
Test temperature 23°C					
1T C(T)	3-1	180.18	194.47	194.47	Valid
1T C(T)	3-2	159	182.68	182.68	Valid
1T C(T)	3-3	130.3	165.37	165.37	Valid
1T C(T)	3-4	208.68	209.28	209.28	Valid
1T C(T)	4-1	258.86	233.09	233.09	Δa >1 mm
1T C(T)	4-3	274.09	239.85	239.85	Δa >1 mm
0.5T C(T)	7-5	205.93	207.90	178.01	Valid

Table 9. MPA fracture toughness measurements of the KS-01 weld

Type of specimen	Specimen ID	Test temperature, °C	K_{Ic}, MPa√m	1T equivalent, MPa√m	Remarks
1T C(T)	XB71	−140	31.00	31.00	
1T C(T)	XB72	−120	33.90	33.90	
2T C(T)	XB85	−103	35.20	38.08	
1T C(T)	XB73	−100	44.40	44.40	
2T C(T)	XB86	−83	44.60	49.25	
1T C(T)	XB74	−80	44.80	44.80	
1T C(T)	XB75	−65	73.58	73.58	K_Q, invalid K_{Ic}
2T C(T)	XB87	−65	46.00	50.92	
2T C(T)	XB88	−48	54.70	61.27	
2T C(T)	XB89	−40	96.70	111.21	K_Q, invalid K_{Ic}

Table 10. Median fracture toughness values of unirradiated KS-01 weld

Test temperature, °C	$K_{Jc(med)}$, Mpa√m	Number of specimens tested, N	Number of valid data, r
−50	88.70	7	7
−35	65.75	8	8
−5	96.71	5	5
23	193.57	7	5

Irradiated fracture toughness specimens were tested from 100°C to 200°C with 25°C intervals to characterize the transition fracture toughness. Only one 0.5T C(T) specimen was intentionally tested at 250°C to ensure a full J-R curve in order to determine J_{Ic} of this material after irradiation. However, the provisional J_Q value of 106 kJ/m^2 from the J-R curve of the irradiated specimen could not be qualified as a valid ASTM E 1820 J_{Ic} value. This test also showed that the material lost almost all its tearing resistance at such a level of embrittlement. Tearing resistance can be characterized by the dimensionless tearing modulus, T_{avg}. The values of tearing modulus were determined from

$$T_{avg} = \frac{E}{\sigma_f^2}\frac{dJ}{da}, \tag{8}$$

where σ_f is the flow stress (the average of the yield strength and ultimate strength) and dJ/da is the average slope of the J-R curve between the exclusion lines. The J-R curve of irradiated specimens becomes practically flat after stable crack growth initiation. The irradiated tearing modulus was only 6. Figure 14 compares two sets of J-R data, the first developed by an unirradiated specimen at 120°C, and the second by an irradiated specimen at 250°C. For comparison, the tearing modulus of the unirradiated specimen is 54.

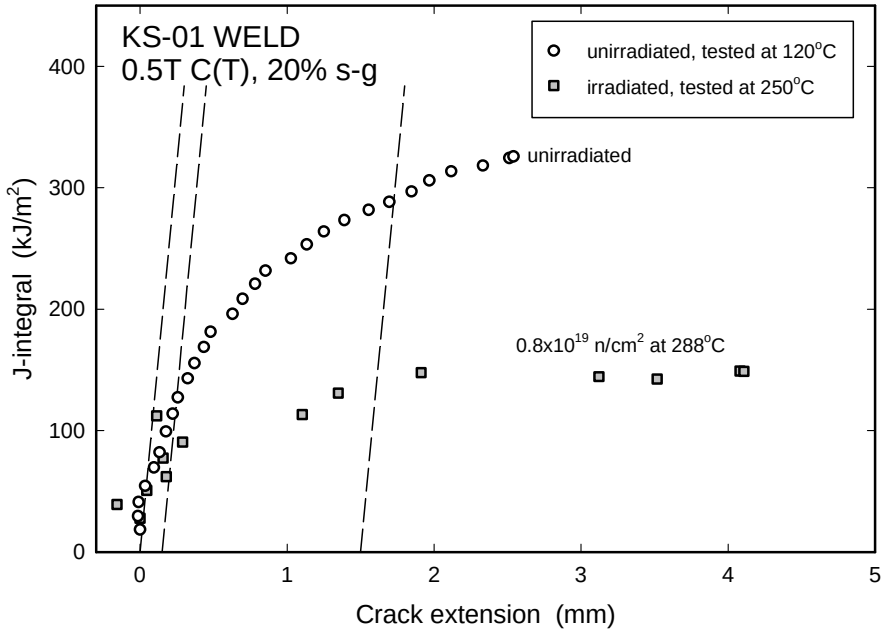

Fig. 14. Comparison of J-R curves developed from unirradiated and irradiated specimens.

Two 1T C(T) specimens, one tested at 175°C and one at 200°C, also developed full J-R curves similar to the J-R curve developed at 250°C by a 0.5T C(T) specimen. In these cases, J_Q values were 116.8 kJ/m^2 and 104.9 kJ/m^2, respectively. Those values could not be qualified as valid J_{Ic} values. Moreover, the final J-integral values from these tests were low, and when converted to their stress-intensity factor values by Eq. (2), they were still smaller than the validity requirement set up by Eq. (6). Following E 1921 guidance, these data were ignored and were not involved in either T_o or $K_{Jc(med)}$ evaluations. In any case, these results indicated that irradiation of the KS-01 weld at 288°C to 0.74×10^{19} neutrons/cm^2 (E >1 MeV) reduced the stable crack growth initiation toughness and significantly diminished the tearing resistance of this material. This leaves a relatively narrow range of temperature within which to examine the shape of the transition curve. Irradiated fracture toughness data are given in Table 11.

After the initial calculation, it was determined that data at 200°C should be excluded from the analysis, since they were outside the $T_o \pm 50$°C range. The final calculation gave the value of T_o equal to 139°C. Thus, the shift of the transition fracture toughness temperature after irradiation of the KS-01 weld at 288°C to 0.8×10^{19}neutrons/cm^2 is 165°C, which is in remarkable agreement with the Charpy T_{41J} shift of 169°C.

It appears that irradiation-induced changes in mechanical and fracture toughness properties of the KS-01 weld are in agreement with general trends for RPV steels [5,16,17], as can be seen in Figs. 15 through 17.

Figure 18 presents fracture toughness data for the KS-01 weld, size-adjusted to 1T before and after irradiation. Master curves are drawn as solid lines, and the 5% and 95% tolerance bounds are drawn as dashed lines. Master curves and tolerance bounds are drawn only within $T_o \pm 50$°C range (89 to 189°C). As in the case of unirradiated data, the 5% and 95% tolerance bounds appear to provide a good description of irradiated fracture toughness data within the temperature range of $T_o \pm$

50°C. However, relatively low energy cleavage fractures that occurred at 200°C (T_o + 61°C) cause concerns regarding the ability of this highly embrittled weld to maintain the master curve shape.

Since there were replicate tests performed at several temperatures, it was decided to determine median fracture toughness values at each of these temperatures and then compare how well those median values follow the master curve. Table 12 presents median fracture toughness values of the irradiated KS-01 weld at different test temperatures, and Fig. 19 presents these values in the unirradiated and irradiated conditions relative to their master curves.

Table 11. Fracture toughness data of the KS-01 weld after irradiation at 288°C to 0.74×10^{19} neutrons/cm^2 (E > 1 MeV)

Type of specimen	Specimen ID	Neutron fluence, 10^{19} neutron/cm^2 (E > 1 MeV)	J_c, kJ/m^2	K_{Jc}, MPa√m	$K_{Jc(1T)}$, MPa√m	Remarks
		Test temperature 100°C				
0.5T C(T)	1-5	0.749	33.33	82.54	72.59	
0.5T C(T)	1-3	0.704	42.78	93.51	81.81	
0.5T C(T)	1-4	0.701	36.04	85.83	75.35	
0.5T C(T)	1-2	0.748	20.5	64.73	57.61	
0.5T C(T)	7-4	0.838	17.67	60.10	53.72	
		Test temperature 125°C				
1T C(T)	2-4	0.780	69.55	118.59	118.59	
1T C(T)	8-13	0.740	28.77	76.27	76.27	
1T C(T)	8-12	0.761	39.85	89.76	89.76	
1T C(T)	8-21	0.701	53.55	104.06	104.06	
1T C(T)	2-3	0.799	39.09	88.90	88.90	
1T C(T)	8-23	0.696	49.69	100.24	100.24	
		Test temperature 150°C				
1T C(T)	8-22	0.704	57.68	107.70	107.70	
1T C(T)	8-31	0.735	54.42	104.61	104.61	
1T C(T)	8-51	0.616	72.98	121.15	121.15	
1T C(T)	8-52	0.627	130.08	161.74	161.74	
1T C(T)	8-43	0.796	67.62	116.61	116.61	
1T C(T)	8-61	0.704	67.49	116.50	116.50	
0.5T C(T)	1-7	0.844	43.15	93.15	81.51	
0.5T C(T)	1-6	0.803	62.16	111.80	97.20	
0.5T C(T)	7-6	0.700	49.17	99.44	86.80	
0.5T C(T)	1-1	0.747	60.37	110.18	95.83	
		Test temperature 175°C				
1T C(T)	8-11	0.756	72.32	119.94	119.94	
1T C(T)	2-2	0.792	101.98	142.42	142.42	
1T C(T)	2-1	0.762	161.6	179.28	142.42	Δa > 1 mm
1T C(T)	8-63	0.731	181	189.74	142.42	Δa > 1 mm
1T C(T)	8-53	0639.	*a*	*a*	*a*	Non-test
		Test temperature 200°C				
1T C(T)	8-62	0.720	*a*	*a*	*a*	Non-test
1T C(T)	8-41	0.760	102.49	141.99	141.99	
1T C(T)	8.32	0.731	73.8	120.49	120.49	
1T C(T)	8-33	0.718	141.76	166.99	120.49	Δa > 1 mm
0.5T C(T)	7-1	0.806	64.96	113.04	98.24	

[a]Full J-R curve; no cleavage.

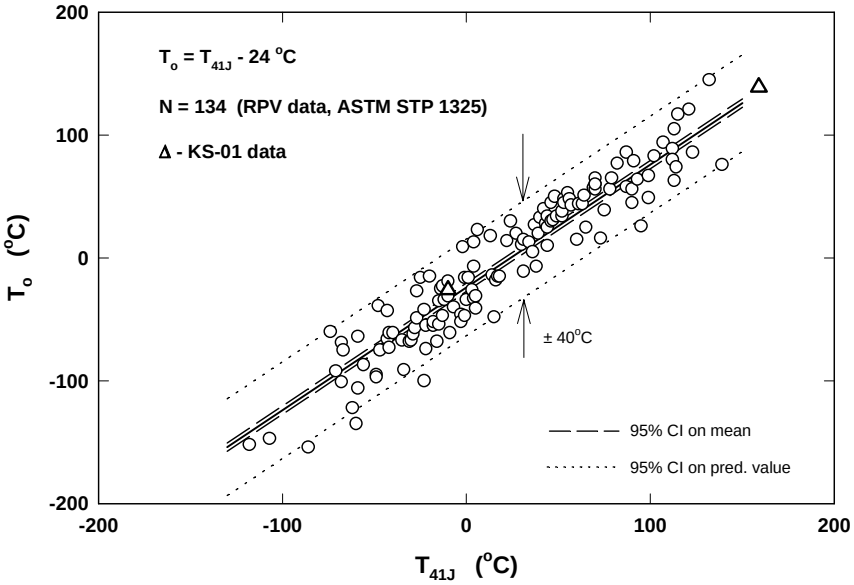

Fig. 15. Relationship between absolute values of T_o and T_{41J} from Ref. [5] and the position of the KS-01 weld in the unirradiated and irradiated conditions.

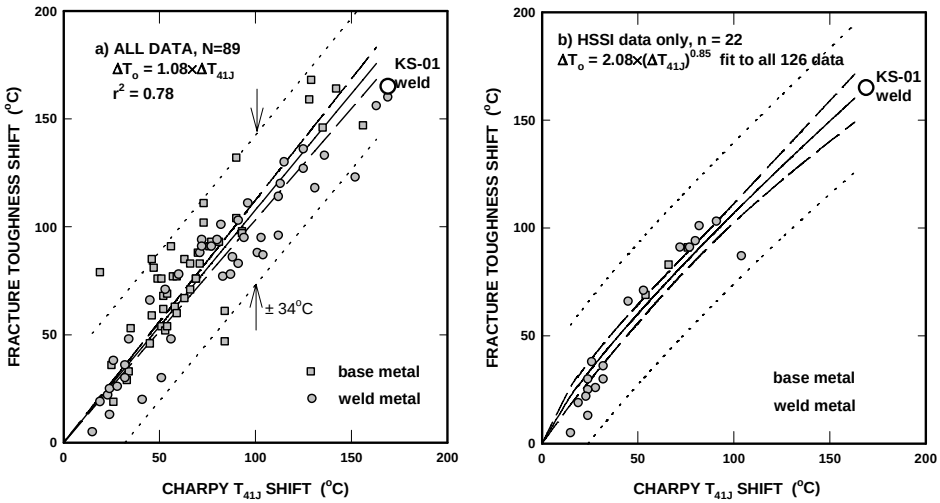

Fig. 16. Relationship between fracture toughness T_o and Charpy T_{41J} shift for RPV steels from Ref. [5] and HSSI data only from Ref. [8] and the position of the KS-01 weld from the present study.

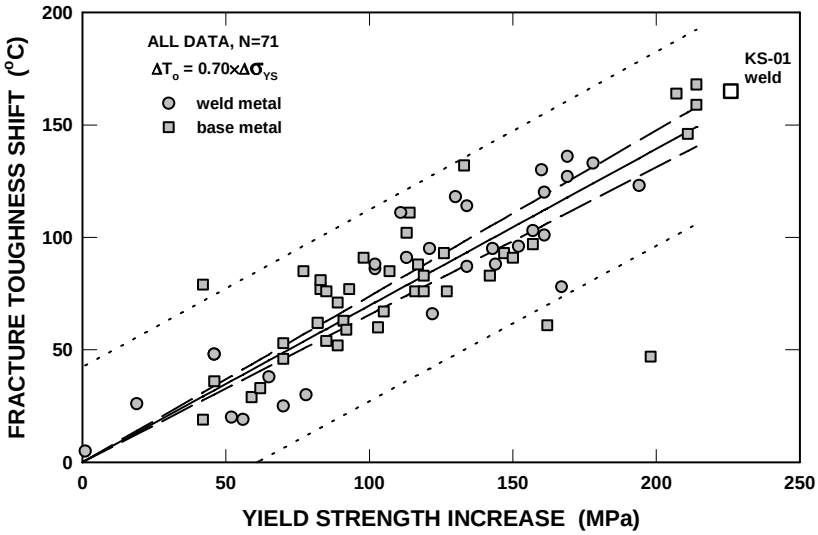

Fig. 17. Relationship between fracture toughness T_o shift and yield strength increase for RPV steels from Ref. [5] and the position of the KS-01 weld from the present study.

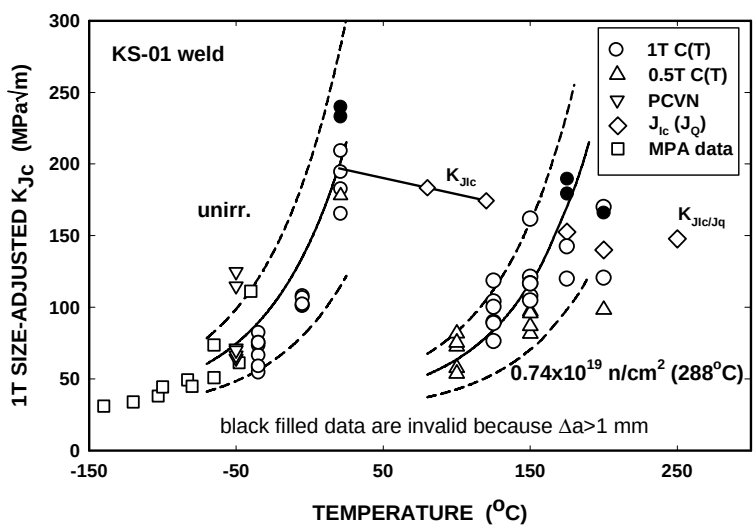

Fig. 18. 1T size-adjusted fracture toughness data of the KS-01 weld before and after irradiation.

Table 12. Median fracture toughness values (adjusted to 1T) for irradiated KS-01 weld

Test temperature, °C	$K_{Jc(med)}$, Mpa√m	Total number of specimens tested, N	Number of E1921 valid data, r
100	66.91	5	5
125	92.72	6	6
150	108.75	10	10
175	147.95	4	2
200	121.68	4	3

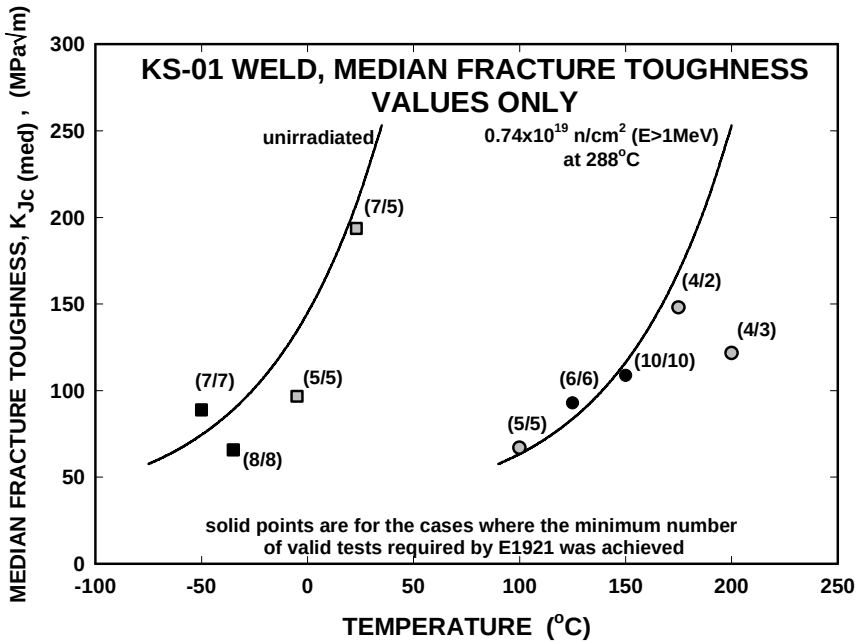

Fig. 19. Median fracture toughness values of the KS-01 weld in the unirradiated and irradiated conditions relative to their master curves. In parenthesis is the number of specimens tested at a given temperature over the number of ASTM E 1921 valid results.

Values for $K_{Jc(med)}$ were calculated by Eq. (5). However, ASTM E 1921 requires a minimum number of valid data points (at least six, depending on the $K_{Jc(med)}$ value) to evaluate $K_{Jc(med)}$. From this point of view, the $K_{Jc(med)}$ values at 100°C and, especially at 175°C and 200°C, fell short of the number of valid data points required by ASTM E 1921. The same pertains to the unirradiated $K_{Jc(med)}$ values at –5°C and 23°C (see Table 10). The numbers in parentheses at each data point in Fig. 19 show the number of specimens tested at that temperature and the number of ASTM E 1921 valid data points.

The present results show that the median fracture toughness values of the irradiated KS-01 weld after a high level of embrittlement tend to follow the master curve shape up to about 148 MPa√m, and then there is a leveling off from the master curve shape. The low ductile initiation toughness (J_Q) did not allow obtaining a statistically significant number of valid cleavage results at 200°C to confirm this statement (two tests had a > 1 mm, see Table 11). However, the repeatable number of low-toughness cleavage fractures at 200°C indicates a potential for deviation of the transition fracture toughness curve from the master curve shape for a highly embrittled RPV weld. Additional studies are envisioned with highly embrittled materials to resolve these issues. As part of this project, small-size specimens, like PCVN, precracked $5 \times 5 \times 27.5$ mm, and 0.4T C(T) specimens would be tested in

the next phase. This proposed testing would be focused at the lower part of the transition region. Atom probe characterization of microstructural changes in the KS-01 weld would also be performed in the next phase.

Summary and Conclusions

Twenty-one 1T C(T) specimens, as well as some CVN and tensile specimens, of the radiation-sensitive KS-01 weld were irradiated in the new HSSI-IAR facilities at the University of Michigan Ford Nuclear Reactor. This weld was produced by MPA-Stuttgart with intentionally high contents of several elements, including copper, nickel, and manganese, to ensure extremely high sensitivity to irradiation. Specimens were irradiated at 288°C to an average fluence of 0.74×10^{19} neutrons/cm^2 (E > 1MeV). The main observations from this study are as follows.

1. The high-strength, radiation-sensitive KS-01 weld exhibited a large Charpy T_{41J} shift of 169°C and a USE drop from 118 J to 78 J due to irradiation. Irradiation also altered the shape of the Charpy transition curve such that the Charpy T_{68J} shift, 217°C, was much larger than the T_{41J} shift.
2. Yield strength increased from 600 MPa to 826 MPa as a result of irradiation.
3. Master curve analysis indicated a fracture toughness T_o shift of 165°C, which is in remarkable agreement with the Charpy T_{41J} shift.
4. Despite a high level of embrittlement and hardening, relationships between embrittlement and hardening of the KS-01 weld follow the general trend for RPV steels.
5. This weld exhibited a low ductile initiation toughness (J_Q) after irradiation. It leaves a relatively narrow range of temperature within which to examine the shape of the transition region curve. Irradiated median fracture toughness values up to 148 MPa√m follow the master curve shape. However, low-toughness brittle fractures occurred at temperatures further above T_o (T_o + 61°C) than expected, with a corresponding leveling of the K_{Jc} data from the master curve shape concept.

References

1. J. G. Merkle, K. Wallin, and D. E. McCabe, *Technical Basis for an ASTM Standard on Determining the Reference Temperature, T_o, for Ferritic Steels in the Transition Range*, NUREG/CR-5504, ORNL/TM-13631, Oak Ridge National Laboratory, Oak Ridge, Tennessee, 1998.
2. U. E. Kaun and F. K. A. Koehring, "Investigations and Measures to Guarantee the Safety of a Pressurized Water Reactor's Pressure Vessel Against Brittle Fracture," pp. 127–148 in *Radiation Embrittlement of Nuclear Reactor Pressure Vessel Steels: An International Review* (Second Volume), ASTM STP 909, L. E. Steele, Ed., American Society for Testing and Materials, Philadelphia, 1986,.
3. R. K. Nanstad, F. M. Haggag, D. E. McCabe, S. K. Iskander, K. O. Bowman, and B. H. Menke, *Irradiation Effects on Fracture Toughness of Two High-Copper Submerged-Arc Welds, HSSI Series 5*, NUREG/CR-1913, ORNL/TM-12156/V1, Oak Ridge National Laboratory, Oak Ridge, Tennessee, October 1992.
4. R. K. Nanstad, D. E. McCabe, B. H. Menke, S. K. Iskander, and F. M. Haggag, "Effects of Irradiation on K_{Ic} curves for High-Copper Welds," pp. 214–33 in *Effects of Radiation on Materials: 14th International Symposium* (Volume II), ASTM STP 1046, N. H. Packan, R. E. Stoller, and A. S. Kumar, Eds., ASTM, Philadelphia, 1990.
5. M. A. Sokolov and R. K. Nanstad, " Comparison of Irradiation-Induced shifts of K_{Jc} and Charpy Impact Toughness for Reactor Pressure Vessel Steels," pp. 167–190 in *Effects of Radiation on Materials: 18th International Symposium*, ASTM STP 1325, R. K. Nanstad, M. L. Hamilton, F. A. Garner, and A. S. Kumar, Eds., American Society for Testing and Materials, Philadelphia, 1999.
6. "Title 10," *Code of Federal Regulations*, Part 50, U.S. Government Printing Office, Washington, D.C., January 1987.
7. F. W. Stallmann, J. A. Wang, F. B. K. Kam, and B. J. Taylor, *PR-EDB: Power Reactor Embrittlement Data Base, Version 2*, NUREG/CR-4816, ORNL/TM-10328/R2, U.S. Nuclear Regulatory Commission, 1994.
8. M. A. Sokolov and R. K. Nanstad, "*Comparison of Irradiation-Induced Shifts of K_{Jc} and Charpy Impact Toughness for Reactor Pressure Vessel Steels*, NUREG/CR-6609, Oak Ridge National Laboratory, Oak Ridge, Tennessee, 2000.
9. D. W. Heatherly, K. R. Thoms, M. T. Hurst, and G. E. Giles, *Heavy-Section Steel Irradiation Program's Reusable Irradiation Facilities*, NUREG/CR-6779, ORNL/TM-2002/77, ORNL, Oak Ridge, TN, 2002.
10. "Standard Test Methods for Tension Testing of Metallic Materials," ASTM E 8-87a, ASTM, Philadelphia, Annual Book of Standards, Vol. 3.01.
11. "Standard Test Method for Determination of Reference Temperature, T_o, for Ferritic Steels in the Transition Range," ASTM E 1921-02, ASTM, Philadelphia, Annual Book of Standards, Vol. 3.01.
12. "Standard Methods for Notched Bar Impact Testing of Metallic Materials," ASTM E 23-91, ASTM, Philadelphia, Annual Book of Standards, Vol. 3.01.

13. "Standard Practice for Conducting Surveillance Tests for Light-Water Cooled Nuclear Power Reactor Vessels," E706(IF), ASTM E185-98, Philadelphia, Annual Book of Standards, Vol. 12.02.

14. "Standard Test Method for Measurement of Fracture Toughness," ASTM E1820-99a, ASTM, Philadelphia, Annual Book of Standards, Vol. 3.01.

15. "Standard Test Method for Plain-Strain Fracture Toughness of Metallic Materials," ASTM E 399-90, ASTM, Philadelphia, Annual Book of Standards, Vol. 3.01.

16. G. R. Odette, P. M. Lombrozo, and R. A. Wullaert, "Relationship Between Irradiation Hardening and Embrittlement of Pressure Vessel Steels," pp. 840–860 in *Effects of Radiation On Materials: Twelfth International Symposium*, ASTM STP 870, F. A. Garner and J. S. Perrin, Eds., ASTM, Philadelphia, 1985.

17. R. K. Nanstad and R. G. Berggren, "Effects of Irradiation Temperature on Charpy and Tensile Properties of High-Copper, Low Upper-Shelf, Submerged-Arc Welds," pp. 239–267 in *Effects of Radiation on Materials: 16th International Symposium*, ASTM STP 1175, A. S. Kumar, D. S. Gelles, R. K. Nanstad, and E. A. Little, Eds., ASTM, Philadelphia, 1993.

Appendix A. Neutronics Analysis of the First Two HSSI-IAR Metallurgical Capsules

I. Remec, C. A. Baldwin

Introduction

The first two capsules with metallurgical specimens were irradiated in the Heavy Section Steel Irradiation (HSSI) Irradiation-Anneal-Reirradiation-(IAR) facility at the University of Michigan's Ford Nuclear Reactor (FNR) in Ann Arbor, Michigan. The specimens received fast neutron fluence (E > 1 MeV) in the range from ~6.2×10^{18} to 9.9×10^{18} cm^{-2}. The uncertainty associated with the fast neutron fluence and other irradiation parameters is ~7% (1 sigma). In the following, the dosimetry measurements and the analysis are briefly described and the results are presented.

Dosimetry Measurements

The horizontal cross section of the HSSI/University of California, Santa Barbara (UCSB), irradiation facility at FNR is shown schematically in Fig. A.1. Because the location of the facility is close to the corner of the core, the fast neutron flux in the north capsule is about 70% higher than the fast neutron flux in the south capsule.

The metallurgical specimens and the neutron dosimeters loaded in capsule 1 and capsule 2 are shown in Figs. A.2 and A.3. The neutron dosimeters used were iron gradient wires, which were placed in the notches in the metallurgical samples, and standard fission-radiometric dosimetry sets (FRDs), which were located in the holes in the shelves of the capsules. After the irradiation, the gradient wires were cut in several pieces, and the activity of each piece was measured separately.

A standard FRD contains Co, Fe, Ni, Ti, Cu, NpO_2, and UO_2 wires. The Co wire is actually a Co/Al alloy with 0.100 wt % Co. The NpO_2 and UO_2 wires are encapsulated in vanadium. The dosimeter wires are packed in a gadolinium vial with an ~0.89-mm-thick (0.035-in.) wall. The gadolinium vial is put in a stainless steel tube with an outer diameter of 0.58 cm (0.23-in.) and a wall thickness of ~0.038 cm. After the irradiation, the FRDs are opened, and the activity of each dosimeter is measured separately.

The measured specific activities of the dosimeters at the end of irradiation (EOI) are given in Tables A.1 and A.2. The iron and Co/Al wires were also irradiated in the removable dosimetry tubes (RDTs) at the ends of the thermal shield (see Fig. A.1). At each of the two locations, one iron and one Co/Al wire were irradiated and were replaced once during the irradiation. These measurements were not used to determine the neutron flux inside the capsules. The measured activities of the RDT dosimeters are given in Tables A.3 and A.4. The details on the dosimetry measurements can be found in Ref. A.1.

The locations of the dosimeters are given in the coordinate system shown in Fig. A.1. The initial locations of the dosimeters are given. The origin of the coordinate system is located at the intersection of the core side of the thermal (gamma) shield, the vertical plane perpendicular to the core side that divides the irradiation facility into two symmetric parts, and the horizontal "fuel mid-plane," which divides the fuel in two equal parts vertically. The *y*-axis is perpendicular to the core side with the positive direction pointing to the east (away from the core). The *x*-axis is parallel to the core face with the positive direction pointing to the south. The *z*-axis is parallel to the core face with the positive direction pointing up.

During the irradiation, packets of metallurgical specimens were moved to different locations within the capsule (together with the dosimeters inserted in them). The capsules were rotated, and the locations of the capsules were interchanged (e.g., the "south" capsule was moved to the "north" position and vice versa). These movements were done to achieve more uniform distribution of fluence

throughout the packets and specimens. Not all of the specimens were removed at the same time. The detailed irradiation history and the changes of the positions are given in Table A.5.

The Analysis

The analysis followed the methodology established for previous HSSI experiments and the neutronics characterization of the HSSI-IAR facility (Ref. A.2). To determine the best-estimate neutron irradiation exposure parameters, a neutron spectrum adjustment procedure was used that combines the results of transport calculations of the neutron field and measurements using radiometric monitors. The input data consisted of the following:

- neutron fluence rate spectrum from transport calculations at each dosimetry location,
- cross sections for each dosimetry reaction used,
- measured activity of each dosimeter, and
- response function for each irradiation exposure parameter.

For each of the dosimeters used in the experiments, a 47-group neutron spectrum was obtained from the three-dimensional neutron transport calculation described in Ref. A.2. The transport calculations were performed with the TORT code (Ref. A.3).

The cross sections and the covariance matrices for the dosimetry reactions were taken from the CROSS-95 library (Ref. A.4), which uses the 640 energy groups (extended SAND-II structure) and was created from the IRDF-90 and ENDF/B-VI dosimetry files. To account for the gadolinium cover of the FRD sets, a modified set of cross sections was generated. The 640 group cross sections were multiplied by attenuation factors defined as

$$AF = \exp\left(- (D*AV/AT) * TH *CS\right)$$

where

AF	=	attenuation factor,
D	=	density of cover material (7.9004 g/cm^3 for Gd),
AV	=	Avogadro's number,
AT	=	atomic weight (157.25 g for Gd),
TH	=	thickness of the cover (0.89 mm, 35 mils), and
CS	=	total absorption cross section of Gd (taken from the IRDF 90 file).

The above formula is an approximation because it does not consider the geometry of the covers and the dosimeters. However, it has been successfully used in similar applications, and it appears to be reasonably accurate for the current application. The resulting cross sections were combined with the cross sections for the bare dosimeters and were converted to 32 energy groups for use in adjustment runs. Cross-section covariance matrices were also converted to the 32-group structure. The computer code FLXPRO from the LSL-M2 code package (Ref A.5) was used for this purpose.

The neutron flux was not constant during the irradiation, mostly due to the relocation of the packages. Therefore, the measured specific activities were converted into reaction probabilities rather than into reaction rates. Reaction probabilities are reaction rates integrated over time. The conversion to reaction probabilities was performed separately for the three groups of dosimeters. The first group consisted of the dosimeters from packages B, C, D, E, FRD-98-05, and FRD-98-06. The second group included the dosimeters from packages F, G, H, I, J, FRD-98-07, and FRD-98-08. The third group consisted of the dosimeters from packet A. Some dosimeters were irradiated in as many as five locations, and this was accounted for in the conversion by using calculated neutron fluxes for all the

locations. The specific reactor power history was also taken into account. The conversion was done with the computer code ACT from the LSL-M2 code package.

The neutron spectrum covariance matrix used for the adjustment runs was originally calculated for the simulated surveillance capsule position of the Oak Ridge Research Reactor Poolside Facility Metallurgical Experiment (Refs. A.6 and A.7). The original calculation of the fluence variance-covariances covered only the range from 18 MeV to 0.1 MeV. Therefore, two energy groups from 1.0×10^{-5} eV to 0.1 eV and from 0.1 eV to 0.1 MeV were added with large variances of 150% and 75%, respectively, and small correlations of 0.1 and 0.2. The original standard deviations were increased by 50%. The spectrum covariance matrix was converted in the group structure used in the adjustment with the FLXPRO computer code from the LSL-M2 code package. Obviously, the assumed spectrum variance-covariance information is only approximate; however, it is not critical for the analysis because the adjustments were relatively small and because comprehensive dosimetry measurements were available.

The least-squares neutron spectrum adjustment calculations were performed with the LSL-M2 computer code. The adjustment runs were done separately for each capsule. The adjustment provided the adjusted neutron spectrum at each location and the best-estimate neutron exposure parameters. The exposure parameters selected to characterize the irradiation conditions were the neutron fluence with energies greater than 1 MeV, 0.5 MeV, and 0.1 MeV, and the displacements-per-atom (dpa) in iron. The fluences were obtained as sums of group fluences over the corresponding energy ranges. For the dpa calculations, the cross sections from Ref. A.8 were folded with the group fluxes and summed. These exposure parameters were determined for each dosimetry location. Due to the varying neutron flux during the irradiation, the time-integrated irradiation parameters are reported rather than their rates.

Results and Discussion

The analysis of this experiment was complicated by the fact that the packets of metallurgical samples were moved during the irradiation. Besides, the examination of the measurements, combined with the comparison with the calculated reaction probabilities, indicated that several dosimeters in the "north" capsule were not loaded according to the loading plan. This required additional work to complete the analysis. The following changes in positions of dosimeter wires were done: E-CT4 and E-CT1 were interchanged, B and C wires were interchanged, E-CV3 and E-CV1 wires were interchanged, and the orientations of the E-CV1, E-CV2, and E-CV3 wires were changed (i.e., the locations of the left and right ends of the wires were changed). The analysis did not suggest any changes in the positions of the dosimeters in the "south" capsule.

The comparison of calculated and adjusted fast neutron fluences (E > 1 MeV) is presented in Tables A.6 and A.7 for the two irradiation capsules. Typical adjustment in the "north" capsule was ~–7%, with the largest adjustment of ~–8.5%. In the "south" capsule, the adjustments were even smaller and did not exceed –3.7%.

The adjusted fast neutron fluences and dpa's are summarized in the Tables A.8 and A.9. The adjusted irradiation parameters should be used for the interpretation of metallurgical experiments.

The uncertainties obtained from the least-squares adjustment procedure took into account estimated uncertainties of neutron transport calculations and uncertainties of the measured activities. Uncertainties of the best-estimate exposure parameter rates obtained from the adjustment calculations at the locations of the dosimeters were in the range of 2.8% to 4.5% (1 sigma). However, the uncertainties were not accurately propagated through all the computational sequences, and there may be biases, which were not recognized. It is therefore suggested that an uncertainty of 7% (1 sigma) should be associated with the adjusted exposure parameters.

Conclusion

The irradiation exposure parameters for the first two HSSI-IAR capsules were determined at the locations of all the dosimeters irradiated in the capsules. The metallurgical specimens received fast neutron fluence (E > 1 MeV) in the range from ~6.2×10^{18} to 9.9×10^{18} cm^{-2}. The uncertainty associated with the fast neutron fluence and other irradiation parameters is ~7% (1 sigma).

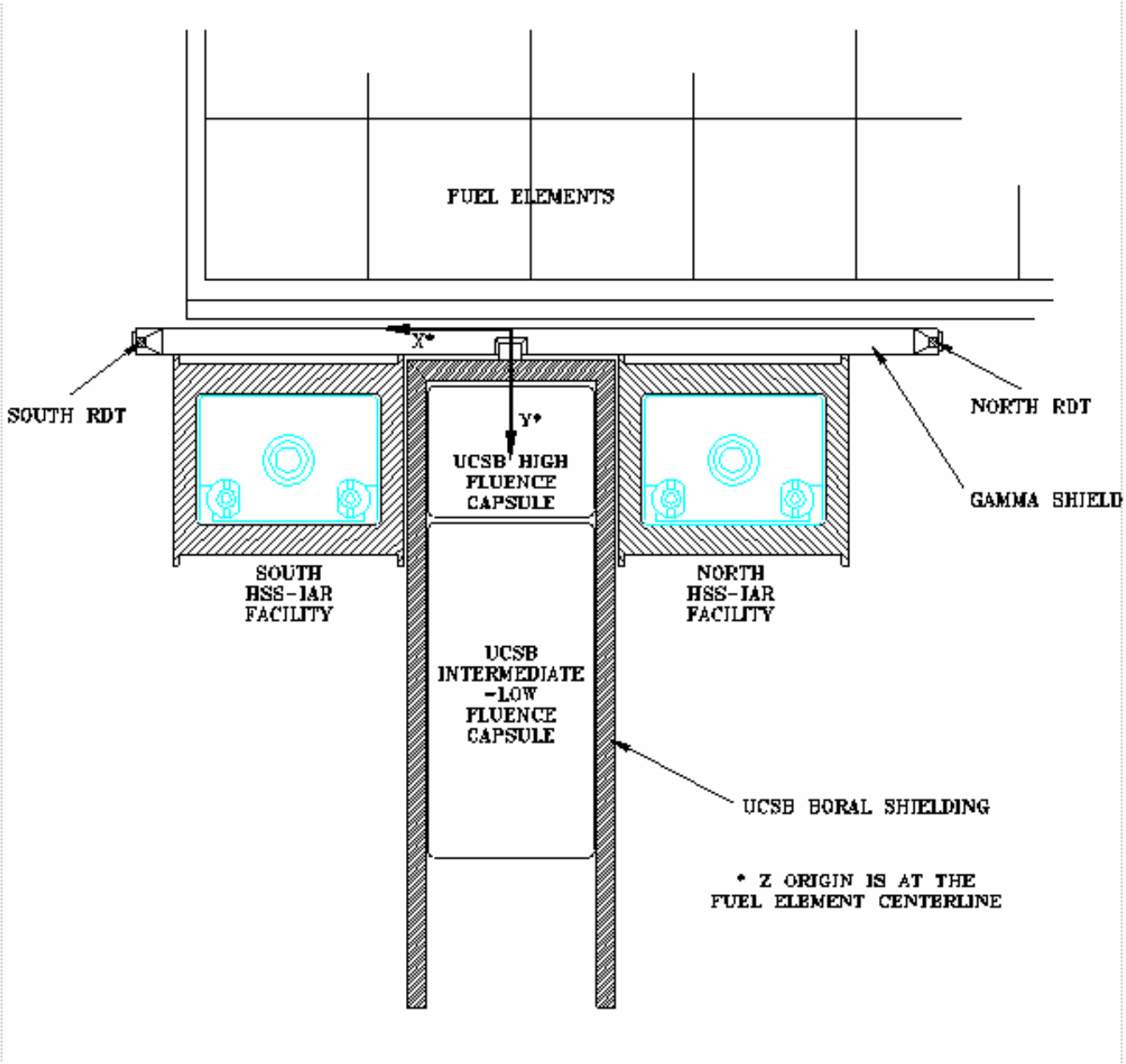

Fig. A.1. Horizontal cross section of the HSSI/UCSB irradiation facility at FNR. The coordinate system used in the report is shown.

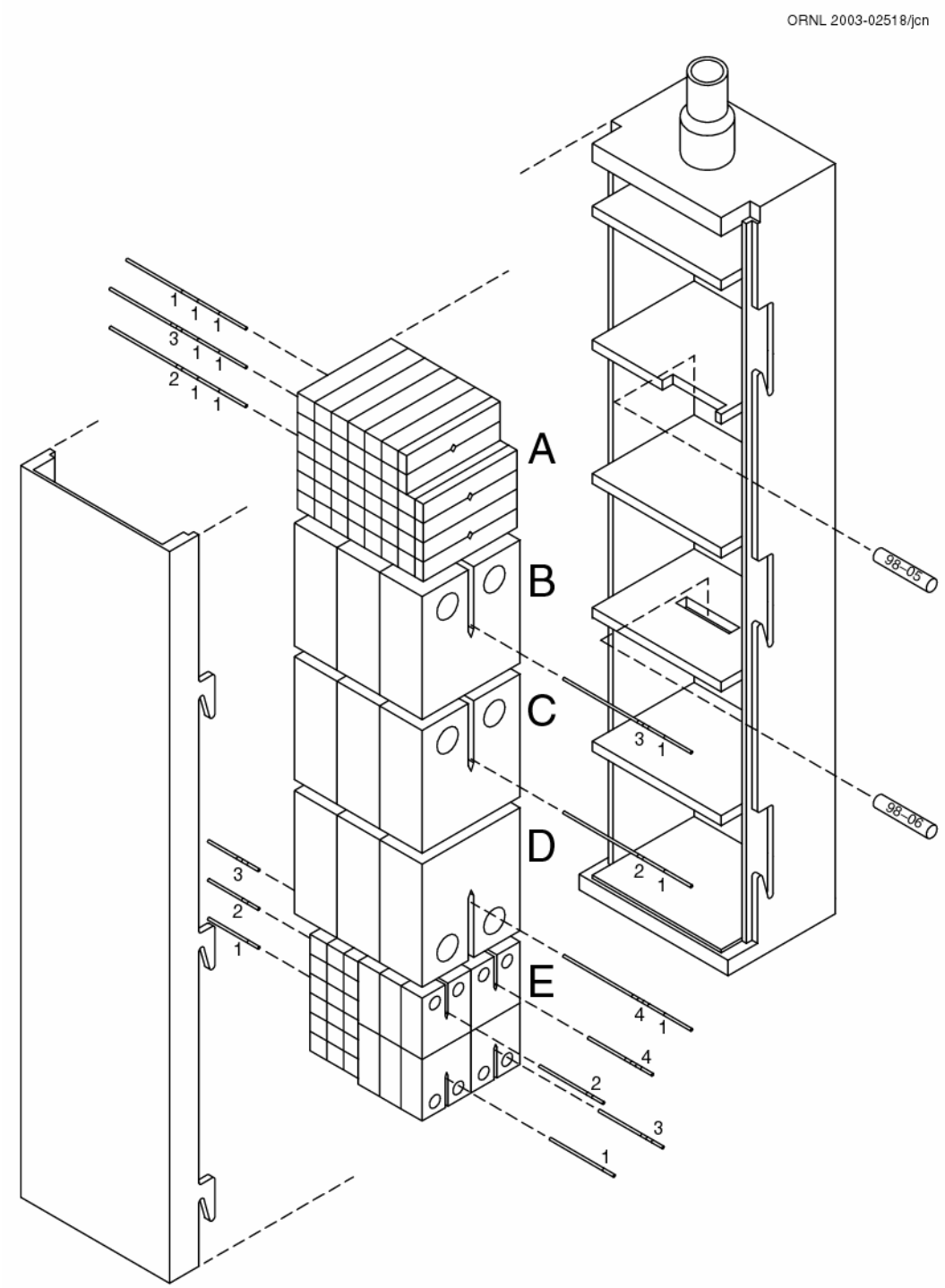

Fig. A.2. Metallurgical specimens and neutron dosimeters loaded in capsule 1, which started irradiation in the north location in the HSSI-IAR facility.

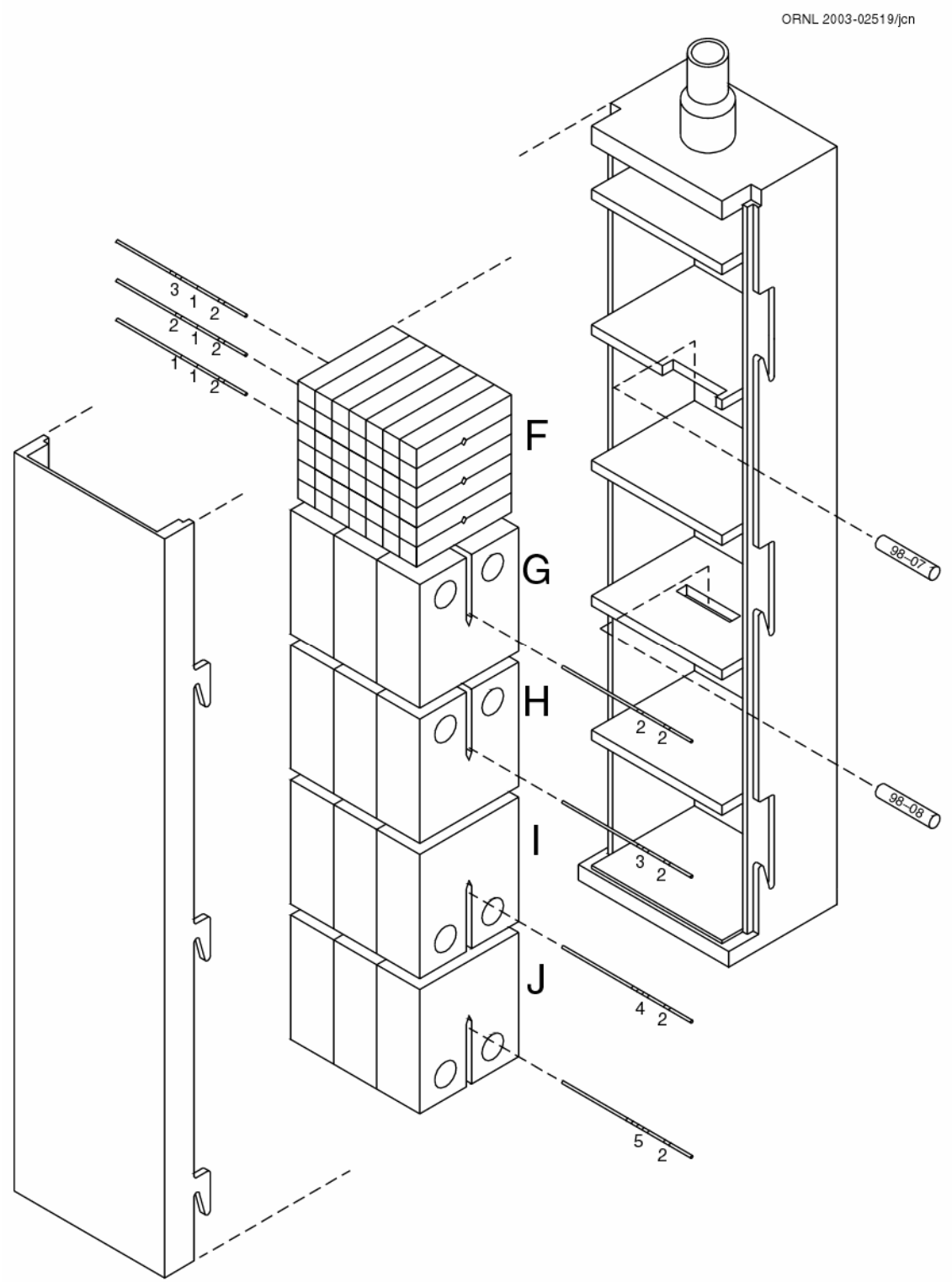

Fig. A.3. Metallurgical specimens and neutron dosimeters loaded in capsule 2, which started irradiation in the south location in the HSSI-IAR facility.

Table A.1. Measured specific activities of the dosimeters in Capsule 1
(which started in the north position in HSSI-IAR Facility)

Dosimeter ID	Reaction	Coordinates X (cm)	Y (cm)	Z (cm)	Activity at EOI (Bq/mg)
A-111-03	FE-54 (N,P) MN-54	−12.201	6.68	16.986	7.31E+03
A-111-02	FE-54 (N,P) MN-54	−10.201	6.68	16.986	7.39E+03
A-111-01	FE-54 (N,P) MN-54	−8.201	6.68	16.986	7.62E+03
A-113-01	FE-54 (N,P) MN-54	−13.701	6.68	14.986	7.18E+03
A-113-02	FE-54 (N,P) MN-54	−12.201	6.68	14.986	7.41E+03
A-113-03	FE-54 (N,P) MN-54	−10.201	6.68	14.986	7.72E+03
A-113-04	FE-54 (N,P) MN-54	−8.201	6.68	14.986	8.00E+03
A-112-01	FE-54 (N,P) MN-54	−13.701	6.68	12.986	7.33E+03
A-112-02	FE-54 (N,P) MN-54	−12.201	6.68	12.986	7.40E+03
A-112-03	FE-54 (N,P) MN-54	−10.201	6.68	12.986	7.69E+03
A-112-04	FE-54 (N,P) MN-54	−8.201	6.68	12.986	8.10E+03
B-13-01	FE-54 (N,P) MN-54	−13.551	6.68	8.712	6.61E+03
B-13-02	FE-54 (N,P) MN-54	−11.011	6.68	8.712	6.61E+03
B-13-03	FE-54 (N,P) MN-54	−8.471	6.68	8.712	6.42E+03
C-12-01	FE-54 (N,P) MN-54	−13.551	6.68	1.803	6.18E+03
C-12-02	FE-54 (N,P) MN-54	−11.011	6.68	1.803	6.08E+03
C-12-03	FE-54 (N,P) MN-54	−8.471	6.68	1.803	6.03E+03
D-14-01	FE-54 (N,P) MN-54	−13.551	6.68	−6.375	6.56E+03
D-14-02	FE-54 (N,P) MN-54	−11.011	6.68	−6.375	6.27E+03
D-14-03	FE-54 (N,P) MN-54	−8.471	6.68	−6.375	6.23E+03
E-CT1-01	FE-54 (N,P) MN-54	−14.186	8.204	−14.554	7.60E+03
E-CT1-02	FE-54 (N,P) MN-54	−12.916	8.204	−14.554	7.69E+03
E-CT1-03	FE-54 (N,P) MN-54	−11.646	8.204	−14.554	7.55E+03
E-CT2-01	FE-54 (N,P) MN-54	−14.186	8.204	−10.744	7.97E+03
E-CT2-02	FE-54 (N,P) MN-54	−12.916	8.204	−10.744	7.95E+03
E-CT2-03	FE-54 (N,P) MN-54	−11.646	8.204	−10.744	7.88E+03
E-CT3-01	FE-54 (N,P) MN-54	−14.186	5.156	−14.554	6.05E+03
E-CT3-02	FE-54 (N,P) MN-54	−12.916	5.156	−14.554	6.02E+03
E-CT3-03	FE-54 (N,P) MN-54	−11.646	5.156	−14.554	5.90E+03
E-CT4-01	FE-54 (N,P) MN-54	−14.186	5.156	−10.744	6.44E+03
E-CT4-02	FE-54 (N,P) MN-54	−12.916	5.156	−10.744	6.37E+03
E-CT4-03	FE-54 (N,P) MN-54	−11.646	5.156	−10.744	6.28E+03
E-CV1-01	FE-54 (N,P) MN-54	−9.701	6.68	−14.649	6.32E+03
E-CV1-02	FE-54 (N,P) MN-54	−8.701	6.68	−14.649	6.46E+03
E-CV1-03	FE-54 (N,P) MN-54	−7.701	6.68	−14.649	6.52E+03

Table A.1 (continued)

Dosimeter ID	Reaction	Coordinates X (cm)	Y (cm)	Z (cm)	Activity at EOI (Bq/mg)
E-CV2-03	FE-54 (N,P) MN-54	−9.701	6.68	−12.649	6.57E+03
E-CV2-02	FE-54 (N,P) MN-54	−8.701	6.68	−12.649	6.64E+03
E-CV2-01	FE-54 (N,P) MN-54	−7.701	6.68	−12.649	6.88E+03
E-CV3-03	FE-54 (N,P) MN-54	−9.701	6.68	−10.649	6.68E+03
E-CV3-02	FE-54 (N,P) MN-54	−8.701	6.68	−10.649	6.77E+03
E-CV3-01	FE-54 (N,P) MN-54	−7.701	6.68	−10.649	6.84E+03
FR-985	CO-59 (N,G) CO-60	−13.616	9.423	11.532	3.76E+03
FR-985	NP-237(N,F) ZR-95	−13.616	9.423	11.532	1.57E+05
FR-985	NP-237(N,F) RU-106	−13.616	9.423	11.532	2.03E+04
FR-985	NP-237(N,F) CS-137	−13.616	9.423	11.532	2.55E+03
FR-985	NP-237(N,F) CE-144	−13.616	9.423	11.532	4.45E+04
FR-985	U-238 (N,F) ZR-95	−13.616	9.423	11.532	2.24E+04
FR-985	U-238 (N,F) RU-106	−13.616	9.423	11.532	4.34E+03
FR-985	U-238 (N,F) CS-137	−13.616	9.423	11.532	3.60E+02
FR-985	U-238 (N,F) CE-144	−13.616	9.423	11.532	7.83E+03
FR-985	NI-58 (N,P) CO-58	−13.616	9.423	11.532	3.40E+05
FR-985	FE-54 (N,P) MN-54	−13.616	9.423	11.532	8.58E+03
FR-985	TI-46 (N,P) SC-46	−13.616	9.423	11.532	4.60E+03
FR-985	CU-63 (N,A) CO-60	−13.616	9.423	11.532	1.18E+02
FR-986	CO-59 (N,G) CO-60	−11.321	6.68	−2.286	3.71E+03
FR-986	NP-237(N,F) ZR-95	−11.321	6.68	−2.286	1.28E+05
FR-986	NP-237(N,F) RU-106	−11.321	6.68	−2.286	2.02E+04
FR-986	NP-237(N,F) CS-137	−11.321	6.68	−2.286	2.52E+03
FR-986	NP-237(N,F) CE-144	−11.321	6.68	−2.286	5.04E+04
FR-986	U-238 (N,F) ZR-95	−11.321	6.68	−2.286	1.66E+04
FR-986	U-238 (N,F) RU-106	−11.321	6.68	−2.286	3.82E+03
FR-986	U-238 (N,F) CS-137	−11.321	6.68	−2.286	3.41E+02
FR-986	U-238 (N,F) CE-144	−11.321	6.68	−2.286	6.81E+03
FR-986	NI-58 (N,P) CO-58	−11.321	6.68	−2.286	2.39E+05
FR-986	FE-54 (N,P) MN-54	−11.321	6.68	−2.286	7.07E+03
FR-986	TI-46 (N,P) SC-46	−11.321	6.68	−2.286	3.26E+03
FR-986	CU-63 (N,A) CO-60	−11.321	6.68	−2.286	9.95E+01

Table A.2. Measured specific activities of the dosimeters in Capsule 2
(which started in the south position in HSSI-IAR Facility)

Dosimeter ID	Reaction	Coordinates			Activity at EOI (Bq/mg)
		X (cm)	Y (cm)	Z (cm)	
F-213-01	FE-54 (N,P) MN-54	8.201	6.68	16.986	6.15E+03
F-213-02	FE-54 (N,P) MN-54	10.201	6.68	16.986	6.36E+03
F-213-03	FE-54 (N,P) MN-54	12.201	6.68	16.986	6.58E+03
F-213-04	FE-54 (N,P) MN-54	13.701	6.68	16.986	6.71E+03
F-212-01	FE-54 (N,P) MN-54	8.201	6.68	14.986	6.43E+03
F-212-02	FE-54 (N,P) MN-54	10.201	6.68	14.986	6.58E+03
F-212-03	FE-54 (N,P) MN-54	12.201	6.68	14.986	6.75E+03
F-212-04	FE-54 (N,P) MN-54	13.701	6.68	14.986	6.98E+03
F-211-01	FE-54 (N,P) MN-54	8.201	6.68	12.986	6.67E+03
F-211-02	FE-54 (N,P) MN-54	10.201	6.68	12.986	6.83E+03
F-211-03	FE-54 (N,P) MN-54	12.201	6.68	12.986	6.96E+03
F-211-04	FE-54 (N,P) MN-54	13.701	6.68	12.986	7.19E+03
G-22-01	FE-54 (N,P) MN-54	8.471	6.68	8.712	6.20E+03
G-22-02	FE-54 (N,P) MN-54	11.011	6.68	8.712	6.34E+03
G-22-03	FE-54 (N,P) MN-54	13.551	6.68	8.712	6.63E+03
H-23-01	FE-54 (N,P) MN-54	8.471	6.68	1.803	5.64E+03
H-23-02	FE-54 (N,P) MN-54	11.011	6.68	1.803	5.80E+03
H-23-03	FE-54 (N,P) MN-54	13.551	6.68	1.803	6.06E+03
I-24-01	FE-54 (N,P) MN-54	8.471	6.68	−6.375	6.11E+03
I-24-02	FE-54 (N,P) MN-54	11.011	6.68	−6.375	6.24E+03
I-24-03	FE-54 (N,P) MN-54	13.551	6.68	−6.375	6.44E+03
J-25-01	FE-54 (N,P) MN-54	8.471	6.68	−13.284	6.30E+03
J-25-02	FE-54 (N,P) MN-54	11.011	6.68	−13.284	6.60E+03
J-25-03	FE-54 (N,P) MN-54	13.551	6.68	−13.284	6.63E+03
FR-987	CO-59 (N,G) CO-60	9.022	9.423	11.532	3.61E+03
FR-987	NP-237(N,F) ZR-95	9.022	9.423	11.532	1.11E+05
FR-987	NP-237(N,F) RU-106	9.022	9.423	11.532	1.86E+04
FR-987	NP-237(N,F) CS-137	9.022	9.423	11.532	2.41E+03
FR-987	NP-237(N,F) CE-144	9.022	9.423	11.532	4.04E+04
FR-987	U-238 (N,F) ZR-95	9.022	9.423	11.532	1.56E+04
FR-987	U-238 (N,F) RU-106	9.022	9.423	11.532	4.04E+03
FR-987	U-238 (N,F) CS-137	9.022	9.423	11.532	3.65E+02
FR-987	U-238 (N,F) CE-144	9.022	9.423	11.532	6.98E+03
FR-987	NI-58 (N,P) CO-58	9.022	9.423	11.532	2.34E+05
FR-987	FE-54 (N,P) MN-54	9.022	9.423	11.532	7.50E+03
FR-987	TI-46 (N,P) SC-46	9.022	9.423	11.532	3.26E+03
FR-987	CU-63 (N,A) CO-60	9.022	9.423	11.532	1.10E+02

Table A.2 (continued)

Dosimeter ID	Reaction	Coordinates			Activity at EOI (Bq/mg)
		X (cm)	Y (cm)	Z (cm)	
FR-988	NP-237(N,F) ZR-95	11.321	6.68	−2.286	1.20E+05
FR-988	CO-59 (N,G) CO-60	11.321	6.68	−2.286	3.87E+03
FR-988	NP-237(N,F) RU-106	11.321	6.68	−2.286	1.93E+04
FR-988	NP-237(N,F) CS-137	11.321	6.68	−2.286	2.55E+03
FR-988	NP-237(N,F) CE-144	11.321	6.68	−2.286	4.92E+04
FR-988	U-238 (N,F) ZR-95	11.321	6.68	−2.286	1.59E+04
FR-988	U-238 (N,F) RU-106	11.321	6.68	−2.286	3.85E+03
FR-988	U-238 (N,F) CS-137	11.321	6.68	−2.286	3.40E+02
FR-988	U-238 (N,F) CE-144	11.321	6.68	−2.286	6.76E+03
FR-988	NI-58 (N,P) CO-58	11.321	6.68	−2.286	2.32E+05
FR-988	FE-54 (N,P) MN-54	11.321	6.68	−2.286	7.16E+03
FR-988	TI-46 (N,P) SC-46	11.321	6.68	−2.286	3.14E+03
FR-988	CU-63 (N,A) CO-60	11.321	6.68	−2.286	1.02E+02

Table A.3. Measured specific activities of the dosimeters from the HSSI-IAR RDTs 07 (North) and 08 (South)

Dosimeter ID	Reaction	Coordinates			Activity at EOI (Bq/mg)
		X (cm)	Y (cm)	Z (cm)	
RDT7-Fe-01	FE-54 (N,P) MN-54	−21.107	0.635	20.955	1.23E+04
RDT7-Fe-02	FE-54 (N,P) MN-54	−21.107	0.635	10.795	1.63E+04
RDT7-Fe-03	FE-54 (N,P) MN-54	−21.107	0.635	0.635	1.79E+04
RDT7-Fe-04	FE-54 (N,P) MN-54	−21.107	0.635	−9.525	1.61E+04
RDT7-Fe-05	FE-54 (N,P) MN-54	−21.107	0.635	−19.685	1.21E+04
RDT7-Co-01	CO-59 (N,G) CO-60	−21.107	0.635	20.955	5.57E+04
RDT7-Co-02	CO-59 (N,G) CO-60	−21.107	0.635	10.795	7.76E+04
RDT7-Co-03	CO-59 (N,G) CO-60	−21.107	0.635	0.635	8.25E+04
RDT7-Co-04	CO-59 (N,G) CO-60	−21.107	0.635	−9.525	7.37E+04
RDT7-Co-05	CO-59 (N,G) CO-60	−21.107	0.635	−19.685	5.26E+04
RDT8-Fe-01	FE-54 (N,P) MN-54	18.418	0.635	20.955	4.77E+03
RDT8-Fe-02	FE-54 (N,P) MN-54	18.418	0.635	10.795	6.23E+03
RDT8-Fe-03	FE-54 (N,P) MN-54	18.418	0.635	0.635	6.45E+03
RDT8-Fe-04	FE-54 (N,P) MN-54	18.418	0.635	−9.525	6.01E+03
RDT8-Fe-05	FE-54 (N,P) MN-54	18.418	0.635	−19.685	4.55E+03
RDT8-Co-01	CO-59 (N,G) CO-60	18.418	0.635	20.955	2.23E+04
RDT8-Co-02	CO-59 (N,G) CO-60	18.418	0.635	10.795	3.04E+04
RDT8-Co-03	CO-59 (N,G) CO-60	18.418	0.635	0.635	3.25E+04
RDT8-Co-04	CO-59 (N,G) CO-60	18.418	0.635	−9.525	2.98E+04
RDT8-Co-05	CO-59 (N,G) CO-60	18.418	0.635	−19.685	2.19E+04

Table A.4. Measured specific activities of the dosimeters from the HSSI-IAR RDTs 09 (North) and 10 (South)

Dosimeter ID	Reaction	Coordinates			Activity at EOI (Bq/mg)
		X (cm)	Y (cm)	Z (cm)	
RDT9-Fe-01	FE-54 (N,P) MN-54	−21.107	0.635	20.955	7.07E+03
RDT9-Fe-02	FE-54 (N,P) MN-54	−21.107	0.635	10.795	9.33E+03
RDT9-Fe-03	FE-54 (N,P) MN-54	−21.107	0.635	0.635	9.38E+03
RDT9-Fe-04	FE-54 (N,P) MN-54	−21.107	0.635	−9.525	1.01E+04
RDT9-Fe-05	FE-54 (N,P) MN-54	−21.107	0.635	−19.685	7.03E+03
RDT9-Co-01	CO-59 (N,G) CO-60	−21.107	0.635	20.955	2.47E+04
RDT9-Co-02	CO-59 (N,G) CO-60	−21.107	0.635	10.795	3.39E+04
RDT9-Co-03	CO-59 (N,G) CO-60	−21.107	0.635	0.635	3.44E+04
RDT9-Co-04	CO-59 (N,G) CO-60	−21.107	0.635	−9.525	3.67E+04
RDT9-Co-05	CO-59 (N,G) CO-60	−21.107	0.635	−19.685	2.51E+04
RDT10-Fe-01	FE-54 (N,P) MN-54	18.418	0.635	20.955	2.30E+03
RDT10-Fe-02	FE-54 (N,P) MN-54	18.418	0.635	10.795	2.86E+03
RDT10-Fe-03	FE-54 (N,P) MN-54	18.418	0.635	0.635	3.15E+03
RDT10-Fe-04	FE-54 (N,P) MN-54	18.418	0.635	−9.525	2.83E+03
RDT10-Fe-05	FE-54 (N,P) MN-54	18.418	0.635	−19.685	2.15E+03
RDT10-Co-01	CO-59 (N,G) CO-60	18.418	0.635	20.955	9.23E+03
RDT10-Co-02	CO-59 (N,G) CO-60	18.418	0.635	10.795	1.27E+04
RDT10-Co-03	CO-59 (N,G) CO-60	18.418	0.635	0.635	1.33E+04
RDT10-Co-04	CO-59 (N,G) CO-60	18.418	0.635	−9.525	1.22E+04
RDT10-Co-05	CO-59 (N,G) CO-60	18.418	0.635	−19.685	9.32E+03

Table A.5. Irradiation history for the HSS-IAR1 capsule (which started in north position) and HSS-IAR2 capsule (which started in south position) [a]
Core power = 2.00 MW

Irradiation interval				Interval duration (EFPH)[b]	Cumulative irradiation time (CFPH)[b]
Start		End			
Date	Time	Date	Time		
Start of irradiation, RDTs 07 and 08 inserted					
12-16-98	10:55	12-23-98	15:19	172.40	172.40
1-12-99	18:19	1-22-99	15:41	237.37	409.77
1-27-99	15:22	2-1-99	11:00	115.63	525.40
2-4-99	11:18	2-5-99	15:20	28.03	553.43
2-9-99	14:30	2-10-99	22:05	31.58	585.02
2-11-99	10:24	2-19-99	15:20	196.93	781.95
2-23-99	19:04	2-25-99	12:55	41.85	823.80
2-25-99	13:25	3-4-99	4:12	158.78	982.58
3-4-99	10:02	3-5-99	15:29	29.45	1012.03
3-10-99	9:56	3-19-99	15:20	221.40	1233.43
HSS-IAR1 metallurgical specimen packets translated to new positions					
Packet A originally in cell 1 moved to cell 3					
Packet C originally in cell 3 moved to cell 1					
Packet D originally in cell 4 moved to cell 5					
Packet E originally in cell 5 moved to cell 4					
HSS-IAR1 and HSS-IAR2 capsules rotated in place 180°					
3-25-99	14:00	4-1-99	7:05	161.08	1394.52
4-6-99	21:41	4-16-99	14:53	233.20	1627.72
4-22-99	9:37	4-23-99	4:15	18.63	1646.35
4-28-99	10:48	4-30-99	11:45	48.95	1695.30
5-4-99	20:29	5-14-99	15:17	234.80	1930.10
HSS-IAR2 metallurgical specimen packets translated to new positions					
Packet F originally in cell 1 moved to cell 3					
Packet H originally in cell 3 moved to cell 1					
Packet I originally in cell 4 moved to cell 5					
Packet J originally in cell 5 moved to cell 4					
5-19-99	14:24	5-28-99	14:44	216.33	2146.43
6-4-99	14:40	6-4-99	16:10	1.50	2147.93
6-4-99	16:27	6-6-99	11:38	43.18	2191.12
6-6-99	13:37	6-9-99	14:26	72.82	2263.93
6-15-99	23:03	6-20-99	5:05	102.03	2365.97
6-20-99	5:24	6-20-99	16:04	10.67	2376.63
6-20-99	21:23	6-25-99	15:30	114.12	2490.75

Table A.5 (continued)

Irradiation interval				Interval duration (EFPH)[b]	Cumulative irradiation time (CFPH)[b]
Start		End			
Date	Time	Date	Time		
7-16-99	11:48	7-20-99	9:40	93.87	2584.62
7-20-99	11:58	7-21-99	10:02	22.07	2606.68
7-21-99	12:25	7-23-99	15:30	51.08	2657.77
7-27-99	17:30	7-30-99	20:25	74.92	2732.68
8-2-99	10:57	8-2-99	13:49	2.87	2735.55
8-2-99	14:41	8-4-99	20:16	53.58	2789.13
8-4-99	20:49	8-6-99	15:45	42.93	2832.07
8-10-99	14:37	8-14-99	18:03	99.43	2931.50
8-14-99	18:36	8-17-99	21:07	74.52	3006.02
8-17-99	21:24	8-19-99	17:45	44.35	3050.37
HSS-IAR1 metallurgical specimen packets removed Packet C in cell 1 recovered and replaced with a dummy Packet B in cell 2 recovered and replaced with a dummy Packet E in cell 4 recovered and replaced with a dummy Packet D in cell 5 recovered and replaced with a dummy HSS-IAR1 FRDs 98-05 and 98-06 recovered RDTs 07 and 08 recovered and replaced with RDTs 09 and 10 HSS-IAR1 moved from the north position to the south position, no rotation HSS-IAR2 moved from the south position to the north position, no rotation					
8-24-99	19:09	8-29-99	14:51	115.70	3166.07
8-29-99	15:10	9-3-99	15:30	120.33	3286.40
9-7-99	21:10	9-15-99	5:43	176.55	3462.95
9-15-99	6:14	9-17-99	14:00	55.77	3518.72
9-21-99	18:41	9-27-99	9:50	135.15	3653.87
9-27-99	18:36	9-30-99	1:46	55.17	3709.03
HSS-IAR2 rotated 180 degrees					
10-5-99	14:27	10-5-99	14:32	0.08	3709.12
10-6-99	11:00	10-8-99	21:46	58.77	3767.88
10-8-99	22:14	10-9-99	15:10	16.93	3784.82
10-9-99	15:45	10-9-99	15:57	0.20	3785.02
10-9-99	18:54	10-10-99	20:00	25.10	3810.12
10-11-99	15:27	10-15-99	15:33	96.10	3906.22
10-19-99	13:28	10-20-99	15:19	25.85	3932.07
10-20-99	15:55	10-24-99	21:54	1.98	4034.05
10-25-99	15:21	10-25-99	15:24	0.05	4034.10
10-25-99	15:43	10-29-99	15:20	95.62	4129.72
11-10-99	17:50	11-12-99	9:0	39.17	4168.88
11-12-99	17:36	11-13-99	3:29	9.88	4178.77
11-13-99	10:00	11-19-99	15:47	49.78	4328.55

Table A.5 (continued)

HSS-IAR1 metallurgical specimen packet A recovered from cell 3
HSS-IAR2 metallurgical specimen packets removed
Packet H in cell 1 recovered
Packet G in cell 2 recovered
Packet F in cell 3 recovered
Packet J in cell 4 recovered
Packet I in cell 5 recovered
HSS-IAR2 FRDs 98-07 and 98-08 recovered
RDTs 09 and 10 recovered
End of Irradiation

[a]For each irradiation period, the date and time for the beginning and the end are given, as well as the duration of the interval in hours and the cumulative irradiation time in hours.

[b]EFPH: effective full-power hours; CFPH: cumulative full-power hours.

Table A.6. Calculated and adjusted fast-neutron fluence (E > 1 MeV) for the dosimeters located in capsule 1 (which started in the north position in HSSI-IAR facility)

Dosimeter ID	Coordinates			Calculated E > 1 MeV (cm^{-2})	Adjusted E > 1 MeV (cm^{-2})	(A-C)/C (%)
	X (cm)	Y (cm)	Z (cm)			
A-111-03	−12.201	6.68	16.986	9.70E+18	9.11E+18	−6.1
A-111-02	−10.201	6.68	16.986	9.97E+18	9.27E+18	−7.1
A-111-01	−8.201	6.68	16.986	1.02E+19	9.38E+18	−7.8
A-113-01	−13.701	6.68	14.986	9.68E+18	9.06E+18	−6.4
A-113-02	−12.201	6.68	14.986	9.94E+18	9.34E+18	−6.0
A-113-03	−10.201	6.68	14.986	1.02E+19	9.61E+18	−6.0
A-113-04	−8.201	6.68	14.986	1.05E+19	9.75E+18	−6.7
A-112-01	−13.701	6.68	12.986	9.86E+18	9.25E+18	−6.2
A-112-02	−12.201	6.68	12.986	1.01E+19	9.48E+18	−6.6
A-112-03	−10.201	6.68	12.986	1.04E+19	9.75E+18	−6.6
A-112-04	−8.201	6.68	12.986	1.07E+19	9.94E+18	−6.8
B-13-01	−13.551	6.68	8.712	8.20E+18	7.56E+18	−7.9
B-13-02	−11.011	6.68	8.712	8.19E+18	7.61E+18	−7.1
B-13-03	−8.471	6.68	8.712	8.05E+18	7.40E+18	−8.0
C-12-01	−13.551	6.68	1.803	7.56E+18	7.01E+18	−7.3
C-12-02	−11.011	6.68	1.803	7.59E+18	7.04E+18	−7.3
C-12-03	−8.471	6.68	1.803	7.53E+18	6.96E+18	−7.6
D-14-01	−13.551	6.68	−6.375	7.86E+18	7.35E+18	−6.5
D-14-02	−11.011	6.68	−6.375	7.87E+18	7.31E+18	−7.2
D-14-03	−8.471	6.68	−6.375	7.76E+18	7.18E+18	−7.4

Table A.6 (continued)

Dosimeter ID	Coordinates X (cm)	Y (cm)	Z (cm)	Calculated E > 1 MeV (cm^{-2})	Adjusted E > 1MeV (cm^{-2})	(A-C)/C (%)
E-CT1-01	−14.186	8.204	−14.554	8.62E+18	7.97E+18	−7.6
E-CT1-02	−12.916	8.204	−14.554	8.62E+18	8.06E+18	−6.5
E-CT1-03	−11.646	8.204	−14.554	8.65E+18	8.03E+18	−7.1
E-CT2-01	−14.186	8.204	−10.744	9.08E+18	8.38E+18	−7.7
E-CT2-02	−12.916	8.204	−10.744	9.06E+18	8.43E+18	−6.9
E-CT2-03	−11.646	8.204	−10.744	9.09E+18	8.44E+18	−7.2
E-CT3-01	−14.186	5.156	−14.554	7.66E+18	7.01E+18	−8.5
E-CT3-02	−12.916	5.156	−14.554	7.60E+18	7.04E+18	−7.4
E-CT3-03	−11.646	5.156	−14.554	7.58E+18	7.00E+18	−7.6
E-CT4-01	−14.186	5.156	−10.744	8.16E+18	7.47E+18	−8.4
E-CT4-02	−12.916	5.156	−10.744	8.11E+18	7.49E+18	−7.6
E-CT4-03	−11.646	5.156	−10.744	8.10E+18	7.48E+18	−7.6
E-CV1-01	−9.701	6.68	−14.649	7.82E+18	7.23E+18	−7.5
E-CV1-02	−8.701	6.68	−14.649	7.73E+18	7.21E+18	−6.7
E-CV1-03	−7.701	6.68	−14.649	7.73E+18	7.15E+18	−7.5
E-CV2-03	−9.701	6.68	−12.649	8.10E+18	7.51E+18	−7.3
E-CV2-02	−8.701	6.68	−12.649	8.00E+18	7.45E+18	−6.8
E-CV2-01	−7.701	6.68	−12.649	8.01E+18	7.46E+18	−6.9
E-CV3-03	−9.701	6.68	−10.649	8.32E+18	7.69E+18	−7.6
E-CV3-02	−8.701	6.68	−10.649	8.22E+18	7.64E+18	−7.0
E-CV3-01	−7.701	6.68	−10.649	8.23E+18	7.58E+18	−7.8
FR-985	−13.616	9.423	11.532	9.06E+18	8.64E+18	−4.6
FR-986	−11.321	6.68	−2.286	8.74E+18	8.34E+18	−4.6

Table A.7. Calculated and adjusted fast-neutron fluence (E > 1 MeV) for the dosimeters located in capsule 2 (which started in the south position in HSSI-IAR facility)

Dosimeter ID	Coordinates			Calculated E > 1 MeV (cm^{-2})	Adjusted E > 1 MeV (cm^{-2})	(A-C)/C (%)
	X (cm)	Y (cm)	Z (cm)			
F-213-01	8.201	6.68	16.986	7.11E+18	7.03E+18	−1.1
F-213-02	10.201	6.68	16.986	7.33E+18	7.29E+18	−0.6
F-213-03	12.201	6.68	16.986	7.55E+18	7.49E+18	−0.8
F-213-04	13.701	6.68	16.986	7.71E+18	7.60E+18	−1.4
F-212-01	8.201	6.68	14.986	7.20E+18	7.25E+18	0.7
F-212-02	10.201	6.68	14.986	7.39E+18	7.46E+18	1.0
F-212-03	12.201	6.68	14.986	7.60E+18	7.64E+18	0.5
F-212-04	13.701	6.68	14.986	7.75E+18	7.77E+18	0.3
F-211-01	8.201	6.68	12.986	7.22E+18	7.39E+18	2.2
F-211-02	10.201	6.68	12.986	7.41E+18	7.60E+18	2.6
F-211-03	12.201	6.68	12.986	7.60E+18	7.75E+18	1.9
F-211-04	13.701	6.68	12.986	7.74E+18	7.87E+18	1.6
G-22-01	8.471	6.68	8.712	7.82E+18	7.60E+18	−2.9
G-22-02	11.011	6.68	8.712	8.02E+18	7.80E+18	−2.7
G-22-03	13.551	6.68	8.712	8.22E+18	7.96E+18	−3.1
H-23-01	8.471	6.68	1.803	6.03E+18	6.16E+18	2.1
H-23-02	11.011	6.68	1.803	6.14E+18	6.27E+18	2.2
H-23-03	13.551	6.68	1.803	6.25E+18	6.39E+18	2.3
I-24-01	8.471	6.68	−6.375	6.88E+18	7.04E+18	2.4
I-24-02	11.011	6.68	−6.375	7.05E+18	7.20E+18	2.3
I-24-03	13.551	6.68	−6.375	7.20E+18	7.31E+18	1.5
J-25-01	8.471	6.68	−13.284	7.84E+18	7.62E+18	−2.8
J-25-02	11.011	6.68	−13.284	8.07E+18	7.92E+18	−2.0
J-25-03	13.551	6.68	−13.284	8.30E+18	7.99E+18	−3.7
FR-987	9.022	9.423	11.532	8.11E+18	8.26E+18	1.9
FR-988	11.321	6.68	−2.286	8.58E+18	8.56E+18	−0.2

Table A.8. Adjusted irradiation parameters at the locations of the dosimeters in capsule 1 (which started in the north position in HSSI-IAR facility)

No.	Location	Fluence of neutrons with energy above			Dpa
		E > 1.0 MeV (cm^{-2})	E > 0.5 MeV (cm^{-2})	E > 0.1 MeV (cm^{-2})	
1	A-111-03	9.106E+18	1.575E+19	2.485E+19	1.369E-02
2	A-111-02	9.268E+18	1.601E+19	2.523E+19	1.392E-02
3	A-111-01	9.381E+18	1.600E+19	2.506E+19	1.399E-02
4	A-113-01	9.059E+18	1.564E+19	2.471E+19	1.362E-02
5	A-113-02	9.342E+18	1.625E+19	2.573E+19	1.409E-02
6	A-113-03	9.613E+18	1.669E+19	2.640E+19	1.448E-02
7	A-113-04	9.748E+18	1.670E+19	2.626E+19	1.458E-02
8	A-112-01	9.248E+18	1.597E+19	2.525E+19	1.391E-02
9	A-112-02	9.475E+18	1.650E+19	2.616E+19	1.431E-02
10	A-112-03	9.748E+18	1.695E+19	2.685E+19	1.470E-02
11	A-112-04	9.937E+18	1.704E+19	2.681E+19	1.487E-02
12	B-13-01	7.556E+18	1.302E+19	2.054E+19	1.133E-02
13	B-13-02	7.605E+18	1.323E+19	2.095E+19	1.147E-02
14	B-13-03	7.401E+18	1.275E+19	2.006E+19	1.109E-02
15	C-12-01	7.008E+18	1.200E+19	1.879E+19	1.045E-02
16	C-12-02	7.041E+18	1.217E+19	1.915E+19	1.056E-02
17	C-12-03	6.956E+18	1.192E+19	1.870E+19	1.038E-02
18	D-14-01	7.350E+18	1.268E+19	2.005E+19	1.105E-02
19	D-14-02	7.305E+18	1.274E+19	2.024E+19	1.104E-02
20	D-14-03	7.179E+18	1.239E+19	1.957E+19	1.079E-02
21	E-CT1-01	7.967E+18	1.344E+19	2.101E+19	1.183E-02
22	E-CT1-02	8.059E+18	1.374E+19	2.159E+19	1.203E-02
23	E-CT1-03	8.034E+18	1.374E+19	2.159E+19	1.201E-02
24	E-CT2-01	8.381E+18	1.414E+19	2.211E+19	1.245E-02
25	E-CT2-02	8.433E+18	1.440E+19	2.263E+19	1.260E-02
26	E-CT2-03	8.438E+18	1.445E+19	2.272E+19	1.263E-02
27	E-CT3-01	7.009E+18	1.198E+19	1.888E+19	1.050E-02
28	E-CT3-02	7.037E+18	1.218E+19	1.930E+19	1.061E-02
29	E-CT3-03	7.004E+18	1.218E+19	1.932E+19	1.058E-02
30	E-CT4-01	7.467E+18	1.275E+19	2.007E+19	1.117E-02
31	E-CT4-02	7.492E+18	1.296E+19	2.052E+19	1.129E-02
32	E-CT4-03	7.477E+18	1.299E+19	2.061E+19	1.129E-02
33	E-CV1-03	7.234E+18	1.256E+19	1.990E+19	1.091E-02
34	E-CV1-02	7.211E+18	1.245E+19	1.967E+19	1.084E-02
35	E-CV1-01	7.148E+18	1.216E+19	1.905E+19	1.067E-02
36	E-CV2-01	7.507E+18	1.304E+19	2.067E+19	1.132E-02
37	E-CV2-02	7.454E+18	1.288E+19	2.035E+19	1.121E-02
38	E-CV2-03	7.458E+18	1.268E+19	1.986E+19	1.113E-02
39	E-CV3-01	7.686E+18	1.336E+19	2.117E+19	1.159E-02
40	E-CV3-02	7.641E+18	1.321E+19	2.087E+19	1.149E-02
41	E-CV3-03	7.581E+18	1.290E+19	2.021E+19	1.131E-02
42	FR-985-C	8.636E+18	1.426E+19	2.192E+19	1.267E-02
43	FR-986-C	8.344E+18	1.453E+19	2.306E+19	1.261E-02

Table A.9. Adjusted irradiation parameters at the locations of the dosimeters in capsule 2 (which started in the south position in HSSI-IAR facility)

No.	Location	Fluence of neutrons with energies above			DPA
		E > 1 MeV (cm^{-2})	E > 0.5 MeV (cm^{-2})	E > 0.1 MeV (cm^{-2})	
1	F-213-01	7.033E+18	1.202E+19	1.886E+19	1.051E-02
2	F-213-02	7.287E+18	1.257E+19	1.981E+19	1.094E-02
3	F-213-03	7.492E+18	1.290E+19	2.033E+19	1.124E-02
4	F-213-04	7.597E+18	1.296E+19	2.037E+19	1.135E-02
5	F-212-01	7.249E+18	1.244E+19	1.959E+19	1.087E-02
6	F-212-02	7.463E+18	1.295E+19	2.051E+19	1.125E-02
7	F-212-03	7.637E+18	1.322E+19	2.093E+19	1.150E-02
8	F-212-04	7.766E+18	1.331E+19	2.099E+19	1.164E-02
9	F-211-01	7.385E+18	1.268E+19	1.998E+19	1.108E-02
10	F-211-02	7.597E+18	1.319E+19	2.090E+19	1.147E-02
11	F-211-03	7.747E+18	1.342E+19	2.125E+19	1.168E-02
12	F-211-04	7.869E+18	1.349E+19	2.128E+19	1.180E-02
13	G-22-01	7.598E+18	1.313E+19	2.075E+19	1.143E-02
14	G-22-02	7.799E+18	1.360E+19	2.161E+19	1.179E-02
15	G-22-03	7.961E+18	1.372E+19	2.167E+19	1.196E-02
16	H-23-01	6.159E+18	1.031E+19	1.601E+19	9.138E-03
17	H-23-02	6.269E+18	1.056E+19	1.643E+19	9.326E-03
18	H-23-03	6.390E+18	1.067E+19	1.655E+19	9.464E-03
19	I-24-01	7.041E+18	1.218E+19	1.935E+19	1.063E-02
20	I-24-02	7.204E+18	1.257E+19	2.004E+19	1.093E-02
21	I-24-03	7.308E+18	1.261E+19	2.002E+19	1.102E-02
22	J-25-01	7.624E+18	1.320E+19	2.094E+19	1.150E-02
23	J-25-02	7.916E+18	1.384E+19	2.205E+19	1.200E-02
24	J-25-03	7.992E+18	1.380E+19	2.189E+19	1.203E-02
25	FR-987-C	8.258E+18	1.379E+19	2.132E+19	1.219E-02
26	FR-988-C	8.557E+18	1.494E+19	2.380E+19	1.298E-02

References

A.1. C. A. Baldwin, Memo to I. Remec, "Dosimetry Counting Results for the First 2 HSSI-IAR Metallurgical Capsules," Dec. 11, 2000.

A.2. I. Remec, C. A. Baldwin, and E. D. Blakeman, *Characterization of the Neutron Field in the HSSI/UCSB Irradiation Facility at the Ford Nuclear Reactor*, NUREG/CR-6646, ORNL/TM-1999/140, submitted to NRC for publication.

A.3. W. A. Rhoades and D. B. Simpson, *The TORT Three-Dimensional Discrete Ordinates Neutron/Photon Transport Code (TORT Version 3)*, ORNL/TM-13221, Oak Ridge National Laboratory, Oak Ridge, Tennessee, October 1997.

A.4. I. Remec and F. B. K. Kam, *An Update of the Dosimetry Cross-Section Data Base for the Adjustment Code LSL-M2*, ORNL-NRC/LTR-95/20, Oak Ridge National Laboratory, Oak Ridge, Tennessee, June 1995.

A.5. F. W. Stallmann, *LSL-M2: A Computer Program for Least-Squares Logarithmic Adjustment of Neutron Spectra*, NUREG/CR-4349, ORNL/TM-9933, Oak Ridge National Laboratory, Oak Ridge, Tennessee, March 1986.

A.6. R. E. Maerker, M. L. Williams, B. L. Broadhead, J. J. Wagschall, and C. V. Fu, *Revision and Extension of the Data Base in the LEPRICON Dosimetry Methodology*, EPRI NP-3841, Electric Power Research Institute, Palo Alto, California, January 1985.

A.7. F. W. Stallmann, *Determination of the Damage Exposure Parameter Values in the PSF Metallurgical Irradiation Experiment*, NUREG/CR-3841, ORNL/TM-9166, U.S. Nuclear Regulatory Commission, Washington, D.C., October 1984.

A.8. I. Remec and J. E. White, *Development of the ENDF/B-VI Atom Displacement Cross Sections for Iron*, ORNL/NRC/LTR-99/4, U. S. Nuclear Regulatory Commission, Washington, D.C., 1999.

Appendix B. Publications List

The work reported here describes materials-irradiation facilities that have been designed, fabricated, and installed by the Oak Ridge National Laboratory (ORNL) Heavy-Section Steel Irradiation (HSSI) Program on behalf of the U.S. Nuclear Regulatory Commission (NRC), Office of Nuclear Regulatory Research. These facilities formed the foundation for generating the data required to provide the NRC with a thorough and quantitative assessment of the effects of neutron irradiation on the material behavior, and in particular, the fracture toughness properties of typical reactor pressure vessel (RPV) steels as they relate to light-water RPV integrity. Results generated from these irradiation experiments are being incorporated into codes and standards that are used to resolve major regulatory issues related to RPV embrittlement, such as pressurized thermal shock, operating pressure-temperature limits, and low-temperature overpressurization. These issues are of particular importance as the nuclear power-plant industry applies for licence extensions that will result in greater accumulated fluence over the lifetime of operation. As part of the HSSI program, the work listed below has enabled the NRC to reduce the uncertainty in its regulatory process with respect to RPV embrittlement, thereby in part allowing the industry to consider license renewal.

This report is a record of work performed at the ORNL under the HSSI Program, which is sponsored by the NRC Office of Nuclear Regulatory Research. A list of publications for the ORNL HSSI Program is given in Sect. B.1.

The HSSI Program includes both follow-on research and the direct continuation of work that was performed under the Heavy-Section Steel Technology (HSST) Program. Previous HSST reports related to irradiation effects in pressure vessel materials and those containing unirradiated properties of materials used in HSSI and HSST irradiation programs are listed in Sect. B.2.

B.1 HSSI Program Reports

1. F. M. Haggag, W. R. Corwin, and R. K. Nanstad, Martin Marietta Energy Systems, Inc., Oak Ridge Natl. Lab., Oak Ridge, Tenn., *Irradiation Effects on Strength and Toughness of Three-Wire Series-Arc Stainless Steel Weld Overlay Cladding*, USNRC Report NUREG/CR-5511 (ORNL/TM-11439), February 1990.

2. L. F. Miller, C. A. Baldwin, F. W. Stallman, and F. B. K. Kam, Martin Marietta Energy Systems, Inc., Oak Ridge Natl. Lab., Oak Ridge, Tenn., *Neutron Exposure Parameters for the Metallurgical Test Specimens in the Sixth Heavy-Section Steel Irradiation Series*, USNRC Report NUREG/CR-5409 (ORNL/TM-11267), March 1990.

3. S. K. Iskander, W. R. Corwin, and R. K. Nanstad, Martin Marietta Energy Systems, Inc., Oak Ridge Natl. Lab., Oak Ridge, Tenn., *Results of Crack-Arrest Tests on Two Irradiated High-Copper Welds*, USNRC Report NUREG/CR-5584 (ORNL/TM-11575), December 1990.

4. R. K. Nanstad and R. G. Berggren, Martin Marietta Energy Systems, Inc., Oak Ridge Natl. Lab., Oak Ridge, Tenn., *Irradiation Effects on Charpy Impact and Tensile Properties of Low Upper-Shelf Welds*, HSSI Series 2 and 3, USNRC Report NUREG/CR-5696 (ORNL/TM-11804), August 1991.

5. R. E. Stoller, Martin Marietta Energy Systems, Inc., Oak Ridge Natl. Lab., Oak Ridge, Tenn., *Modeling the Influence of Irradiation Temperature and Displacement Rate on Radiation-Induced Hardening in Ferritic Steels*, USNRC Report NUREG/CR5859 (ORNL/TM-12073), August 1992.

6. R. K. Nanstad, D. E. McCabe, and R. L. Swain, Martin Marietta Energy Systems, Inc., Oak Ridge Natl. Lab., Oak Ridge, Tenn., *Chemical Composition RTNDT Determinations for Midland Weld WF-70*, USNRC Report NUREG/CR-5914 (ORNL-6740), December 1992.

7. R. K. Nanstad, F. M. Haggag, D. E. McCabe, S. K. Iskander, K. O. Bowman, and B. H. Menke, Martin Marietta Energy Systems, Inc., Oak Ridge Natl. Lab., Oak Ridge, Tenn., *Irradiation Effects on Fracture Toughness of Two High-Copper Submerged-Arc Welds*, USNRC Report NUREG/CR-5913 (ORNL/TM-12156/V1), October 1992.

8. S. K. Iskander, W. R. Corwin, and R. K. Nanstad, Martin Marietta Energy Systems, Inc., Oak Ridge Natl. Lab., Oak Ridge, Tenn., *Crack-Arrest Tests on Two Irradiated High-Copper Welds*, USNRC Report NUREG/CR-6139 (ORNL/TM-12513), March 1994.

9. R. E. Stoller, Martin Marietta Energy Systems, Inc., Oak Ridge Natl. Lab., Oak Ridge, Tenn., *A Comparison of the Relative Importance of Copper Precipitates and Point Defects in Reactor Pressure Vessel Embrittlement*, USNRC Report NUREG/CR-6231 (ORNL/TM-6811), December 1994.

10. D. E. McCabe, R. K. Nanstad, S. K. Iskander, and R. L. Swain, Martin Marietta Energy Systems, Inc., Oak Ridge Natl. Lab., Oak Ridge, Tenn., *Unirradiated Material Properties of Midland Weld WF-70*, USNRC Report NUREG/CR-6249 (ORNL/TM-12777), October 1994.

11. P. M. Rice and R. E. Stoller, Lockheed Martin Energy Systems, Oak Ridge Natl. Lab., Oak Ridge, Tenn., *Microstructural Characterization of Selected AEA/UCSB Model FeCuMn Alloys*, USNRC Report NUREG/CR-6332 (ORNL/TM-12980), June 1996.

12. J. H. Giovanola and J. E. Crocker, SRI International, *Fracture Toughness Testing with Cracked Round Bars: Feasibility Study*, USNRC Report NUREG/CR-6342 (ORNL/SUB/94-DHK60), April 2000.

13. F. M. Haggag and R. K. Nanstad, Lockheed Martin Energy Systems, Oak Ridge Natl. Lab., Oak Ridge, Tenn., Effects of Thermal Aging and Neutron Irradiation on the Mechanical Properties of Three-Wire Stainless Steel Weld Overlay Cladding, USNRC Report NUREG/CR-6363 (ORNL/TM-13047), May 1997.

14. M. A. Sokolov and D. J. Alexander, Lockheed Martin Energy Systems, Oak Ridge Natl. Lab., Oak Ridge, Tenn., *An Improved Correlation Procedure for Subsize and Full-Size Charpy Impact Specimen Data*, USNRC Report NUREG/CR-6379 (ORNL/TM-13088), March 1997.

15. S. K. Iskander and R. E. Stoller, Lockheed Martin Energy Research Corporation, Oak Ridge Natl. Lab., Oak Ridge, Tenn., Results of Charpy V-Notch Impact Testing of Structural Steel Specimens Irradiated at ~30°C to 1×10^6 Neutrons/cm2 in a Commercial Reactor Cavity, USNRC Report NUREG/CR-6399 (ORNL-6886), April 1997.

16. S. K. Iskander, P. P. Milella, and A. Pini, Lockheed Martin Energy Research Corporation, Oak Ridge Natl. Lab., Oak Ridge, Tenn., *Results of Crack-Arrest Tests on Irradiated A 503 Class 3 Steel*, USNRC Report NUREG/CR-6447 (ORNL-6894), February 1998.

17. P. Pareige, K. F. Russell, R. E. Stoller, and M. K. Miller, Lockheed Martin Energy Research Corporation, Oak Ridge Natl. Lab., Oak Ridge, Tenn., *Influence of Long-Term Thermal Aging on the Microstructural Evolution of Nuclear Reactor Pressure Vessel Materials: An Atom Probe Study*, USNRC Report NUREG/CR-6537(ORNL-13406), March 1998.

18. I. Remec, C. A. Baldwin, and F. B. K. Kam, Lockheed Martin Energy Research Corporation, Oak Ridge Natl. Lab., Oak Ridge, Tenn., *Neutron Exposure Parameters for Capsule 10.05 in the Heavy-Section Steel Irradiation Program Tenth Irradiation Series*, USNRC Report NUREG/CR-6600 (ORNL/TM-13548), October 1998.

19. I. Remec, C. A. Baldwin, and F. B. K. Kam, Lockheed Martin Energy Research Corporation, Oak Ridge Natl. Lab., Oak Ridge, Tenn., *Neutron Exposure Parameters for the Dosimetry Capsule in the Heavy-Section Steel Irradiation Program Tenth Irradiation Series*, USNRC Report NUREG/CR-6601 (ORNL/TM-13549), October 1998.

20. D. E. McCabe, R. K. Nanstad, S. K. Iskander, D. W. Heatherly, and R. L. Swain, Lockheed Martin Energy Research Corporation, Oak Ridge Natl. Lab., Oak Ridge, Tenn., *Evaluation of WF-70 Weld Metal from the Midland Unit 1 Reactor Vessel—Final Report*, USNRC Report NUREG/CR-5736 (ORNL/TM-13748), November 2000.

21. Mikhail A. Sokolov and Randy K. Nanstad, Lockheed Martin Energy Research Corporation, Oak Ridge Natl. Lab., Oak Ridge, Tenn., *Comparison of Irradiation-Induced Shifts of K_{Jc} and Charpy Impact Toughness for Reactor Pressure Vessel Steels*, USNRC Report NUREG/CR-6609 (ORNL/TM-13755), November 2000.

22. S. K. Iskander, C. A. Baldwin, D. W. Heatherly, D. E. McCabe, I. Remec, and R. L. Swain, UT-Battelle, LLC, Oak Rdge Nat'l. Lab., Oak Ridge, Tenn., *Detailed Results of Testing Unirradiated and Irradiated Crack-Arrest Toughness Specimens from the Low-Upper-Shelf-Energy, High-Copper Weld, WF-70*, USNRC Report NUREG/CR-6621 (ORNL/TM-13764), to be published (submitted July 2004).

23. D. J. Alexander, K. B. Alexander, M. K. Miller, and R. K. Nanstad, Lockheed Martin Energy Research Corporation, Oak Ridge Natl. Lab., Oak Ridge, Tenn., *The Effect of Aging at 343°C on the Microstructure and Mechanical Properties of Type 308 Stainless Steel Welds*, USNRC Report NUREG/CR-6628 (ORNL/TM-13767), November 2000.

24. M. K. Miller, P. Pariege, K. F. Russell, and R. E. Stoller, Lockheed Martin Energy Research Corporation, Oak Ridge Natl. Lab., Oak Ridge, Tenn., *An Atom Probe Tomography Characterization of the Solute Distributions in a Neutron Irradiated and Annealed Pressure Vessel Steel*, USNRC Report NUREG/CR-6629 (ORNL/TM-13768), November 2000.

25. I. Remec, C. A. Baldwin, and E. D. Blakeman, Lockheed Martin Energy Research Corporation, Oak Ridge Natl. Lab., Oak Ridge, Tenn., *Characterization of the Neutron Field in the HSSI/UCSB Irradiation Facility at the Ford Nuclear Reactor, USNRC Report NUREG/CR-6646* (ORNL/TM-1999/140), to be published (submitted September 1999).

26. P. M. Rice and R. E. Stoller, UT-Battelle, LLC, Oak Ridge Natl. Lab., Oak Ridge, Tenn., *Hardening Behavior of Ferritic Alloys at High Doses and After Thermal Aging*, USNRC Report NUREG/CR-6643 (ORNL/TM-1999/297), to be published (submitted August 2000).

27. S. K. Iskander, J. T. Hutton, L. E. Creech, M. Suzuki, K. Onizawa, E. T. Manneschmidt, R. K. Nanstad, T. M. Rosseel, and P. S. Bishop, UT-Battelle, LLC, Oak Ridge Natl. Lab., Oak Ridge, Tenn., *Attenuation of Charpy Impact Toughness Through the Thickness of a JPDR Pressure Vessel Weldment*, USNRC Report NUREG/CR-6709 (ORNL/TM-2000-343), to be published (submitted January 2001).

28. K. Onizawa, E. van Walle, W. Pavinich, and R. K. Nanstad, UT-Battelle, LLC, Oak Ridge Natl. Lab., Oak Ridge, Tenn., *Results and Analysis of The ASTM Round Robin On Reconstitution*, USNRC Report NUREG/CR-6777, (ORNL/TM-2001/34) August 2002.

29. D. W. Heatherly, K. R. Thoms, M. T. Hurst, and G. E. Giles, UT-Battelle, LLC, Oak Ridge Natl. Lab., Oak Ridge, Tenn., *Heavy-Section Steel Irradiation Program's Reusable Irradiation Facilities*, USNRC Report NUREG/CR-6779, (ORNL/TM-2002/77) to be published (submitted February 2002).

30. R. K. Nanstad and D. E. McCabe, UT-Battelle, LLC, Oak Ridge Natl. Lab., Oak Ridge, Tenn., Preliminary Evaluation of Precracked Charpy Specimens for Determining Fracture Toughness of Reactor Pressure Vessel Weldment, New Coordinated Research Program, USNRC Report NUREG/CR-XXXX (ORNL/TM-2001/YYY), to be published (submitted July 2001).

31. M. A. Sokolov, R. K. Nanstad, I. Remec, C. A. Baldwin, and R. L. Swain, UT-Battelle, LLC, Oak Ridge Natl. Lab., Oak Ridge, Tenn., *Fracture Toughness of an Irradiated, Highly Embrittled Reactor Pressure Vessel Weld*, USNRC Report NUREG/CR-XXXX (ORNL/TM-2002/293), to be published (submitted December 2003).

32. M. K. Miller et al., UT-Battelle, LLC, Oak Ridg Natl. Lab., Oak Ridge, Tenn., *APT Characterization of Highly Irradiated High-Nickel RPV Welds and Low-Upper-Shelf Midland Weld Materials*, USNRC Report NUREG/CR-XXXX, ORNL/TM-200X/XXX), to be published.

33. M. A. Sokolov et al., UT-Battelle, LLC, Oak Ridg Natl. Lab., Oak Ridge, Tenn., *The Effects of Radiation on Fracture Toughness Curve Shape on a Low-Upper-Shelf Weld*, USNRC Report NUREG/CR-XXXX, ORNL/TM-200X/XXX), to be published.

B.2 Reports Related to Irradiation Effects in Pressure Vessel Materials and to the Properties of Unirradiated Materials Used in the HSSI and HSST Programs

C. E. Childress, Union Carbide Corp. Nuclear Div., Oak Ridge Natl. Lab., Oak Ridge, Tenn., Fabrication History of the First Two 12-in.-Thick A-533 Grade B, Class 1 Steel Plates of the Heavy-Section Steel Technology Program, ORNL-4313, February 1969.

T. R. Mager and F. O. Thomas, Westinghouse Electric Corporation, PWR Systems Division, Pittsburgh, Pa., *Evaluation by Linear Elastic Fracture Mechanics of Radiation Damage to Pressure Vessel Steels*, WCAP-7328 (Rev.), October 1969.

P. N. Randall, TRW Systems Group, Redondo Beach, Calif., *Gross Strain Measure of Fracture Toughness of Steels*, HSSTP-TR-3, Nov. 1, 1969.

L. W. Loechel, Martin Marietta Corporation, Denver, Colo., *The Effect of Testing Variables on the Transition Temperature in Steel*, MCR-69-189, Nov. 20, 1969.

W. O. Shabbits, W. H. Pryle, and E. T. Wessel, Westinghouse Electric Corporation, PWR Systems Division, Pittsburgh, Pa., *Heavy-Section Fracture Toughness Properties of A533 Grade B Class 1 Steel Plate and Submerged Arc Weldment*, WCAP-7414, December 1969.

C. E. Childress, Union Carbide Corp. Nuclear Div., Oak Ridge Natl. Lab., Oak Ridge, Tenn., *Fabrication History of the Third and Fourth ASTM A-533 Steel Plates of the Heavy-Section Steel Technology Program*, ORNL-4313-2, February 1970.

P. B. Crosley and E. J. Ripling, Materials Research Laboratory, Inc., Glenwood, Ill., *Crack Arrest Fracture Toughness of A533 Grade B Class 1 Pressure Vessel Steel*, HSSTP-TR-8, March 1970.

F. J. Loss, Naval Research Laboratory, Washington, D.C., Dynamic *Tear Test Investigations of the Fracture Toughness of Thick-Section Steel*, NRL-7056, May 14, 1970.

T. R. Mager, Westinghouse Electric Corporation, PWR Systems Division, Pittsburgh, Pa., *Post-Irradiation Testing of 2T Compact Tension Specimens*, WCAP-7561, August 1970.

F. J. Witt and R. G. Berggren, Union Carbide Corp. Nuclear Div., Oak Ridge Natl. Lab., Oak Ridge, Tenn., *Size Effects and Energy Disposition in Impact Specimen Testing of ASTM A533 Grade B Steel*, ORNL/TM-3030, August 1970.

D. A. Canonico, Union Carbide Corp. Nuclear Div., Oak Ridge Natl. Lab., Oak Ridge, Tenn., *Transition Temperature Considerations for Thick-Wall Nuclear Pressure Vessels*, ORNL/TM-3114, October 1970.

T. R. Mager, Westinghouse Electric Corporation, PWR Systems Division, Pittsburgh, Pa., *Fracture Toughness Characterization Study of A533, Grade B, Class 1 Steel*, WCAP-7578, October 1970.

W. O. Shabbits, Westinghouse Electric Corporation, PWR Systems Division, Pittsburgh, Pa., *Dynamic Fracture Toughness Properties of Heavy-Section A533 Grade B Class 1 Steel Plate*, WCAP-7623, December 1970.

C. E. Childress, Union Carbide Corp. Nuclear Div., Oak Ridge Natl. Lab., Oak Ridge, Tenn., Fabrication Procedures and Acceptance Data for ASTM A-533 Welds and a 10-in.-Thick ASTM A-543 Plate of the Heavy Section Steel Technology Program, ORNL-TM-4313-3, January 1971.

D. A. Canonico and R. G. Berggren, Union Carbide Corp. Nuclear Div., Oak Ridge Natl. Lab., Oak Ridge, Tenn., *Tensile and Impact Properties of Thick-Section Plate and Weldments*, ORNL/TM-3211, January 1971.

C. W. Hunter and J. A. Williams, Hanford Eng. Dev. Lab., Richland, Wash., *Fracture and Tensile Behavior of Neutron-Irradiated A533-B Pressure Vessel Steel*, HEDL-TME-71-76, Feb. 6, 1971.

C. E. Childress, Union Carbide Corp. Nuclear Div., Oak Ridge Natl. Lab., Oak Ridge, Tenn., *Manual for ASTM A533 Grade B Class 1 Steel (HSST Plate 03) Provided to the International Atomic Energy Agency*, ORNL/TM-3193, March 1971.

P. N. Randall, TRW Systems Group, Redondo Beach, Calif., *Gross Strain Crack Tolerance of A533-B Steel*, HSSTP-TR-14, May 1, 1971.

C. L. Segaser, Union Carbide Corp. Nuclear Div., Oak Ridge Natl. Lab., Oak Ridge, Tenn., Feasibility Study, Irradiation of Heavy-Section Steel Specimens in the South Test Facility of the Oak Ridge Research Reactor, ORNL/TM-3234, May 1971.

H. T. Corten and R. H. Sailors, University of Illinois, Urbana, Ill., Relationship Between Material Fracture Toughness Using Fracture Mechanics and Transition Temperature Tests, T&AM Report 346, Aug. 1, 1971.

L. A. James and J. A. Williams, Hanford Eng. Dev. Lab., Richland, Wash., Heavy Section Steel Technology Program Technical Report No. 21, The Effect of Temperature and Neutron Irradiation Upon the Fatigue-Crack Propagation Behavior of ASTM A533 Grade B, Class 1 Steel, HEDL-TME 72-132, September 1972.

P. B. Crosley and E. J. Ripling, Materials Research Laboratory, Inc., Glenwood, Ill., *Crack Arrest in an Increasing K-Field*, HSSTP-TR-27, January 1973.

W. J. Stelzman and R. G. Berggren, Union Carbide Corp. Nuclear Div., Oak Ridge Natl. Lab., Oak Ridge, Tenn., *Radiation Strengthening and Embrittlement in Heavy-Section Steel Plates and Welds*, ORNL-4871, June 1973.

J. M. Steichen and J. A. Williams, Hanford Eng. Dev. Lab., Richland, Wash., *High Strain Rate Tensile Properties of Irradiated ASTM A533 Grade B Class 1 Pressure Vessel Steel*, HEDL-TME 73-74, July 1973.

J. A. Williams, Hanford Eng. Dev. Lab., Richland, Wash., The Irradiation and Temperature Dependence of Tensile and Fracture Properties of ASTM A533, Grade B, Class 1 Steel Plate and Weldment, HEDL-TME 73-75, August 1973.

J. A. Williams, Hanford Eng. Dev. Lab., Richland, Wash., Some Comments Related to the Effect of Rate on the Fracture Toughness of Irradiated ASTM A553-B Steel Based on Yield Strength Behavior, HEDL-SA 797, December 1974.

J. A. Williams, Hanford Eng. Dev. Lab., Richland, Wash., The Irradiated Fracture Toughness of ASTM A533, Grade B, Class 1 Steel Measured with a Four-Inch-Thick Compact Tension Specimen, HEDL-TME 75-10, January 1975.

J. G. Merkle, G. D. Whitman, and R. H. Bryan, Union Carbide Corp. Nuclear Div., Oak Ridge Natl. Lab., Oak Ridge, Tenn., *An Evaluation of the HSST Program Intermediate Pressure Vessel Tests in Terms of Light-Water-Reactor Pressure Vessel Safety*, ORNL/TM-5090, November 1975.

J. A. Davidson, L. J. Ceschini, R. P. Shogan, and G. V. Rao, Westinghouse Electric Corporation, Pittsburgh, Pa., *The Irradiated Dynamic Fracture Toughness of ASTM A533, Grade B, Class 1 Steel Plate and Submerged Arc Weldment*, WCAP-8775, October 1976.

J. A. Williams, Hanford Eng. Dev. Lab., Richland, Wash., *Tensile Properties of Irradiated and Unirradiated Welds of A533 Steel Plate and A508 Forgings*, NUREG/CR-1158 (ORNL/SUB-79/50917/2), July 1979.

J. A. Williams, Hanford Eng. Dev. Lab., Richland, Wash., T*he Ductile Fracture Toughness of Heavy-Section Steel Plate*, NUREG/CR-0859, September 1979.

K. W. Carlson and J. A. Williams, Hanford Eng. Dev. Lab., Richland, Wash., *The Effect of Crack Length and Side Grooves on the Ductile Fracture Toughness Properties of ASTM A533 Steel*, NUREG/CR-1171 (ORNL/SUB-79/50917/3), October 1979.

G. A. Clarke, Westinghouse Electric Corp., Pittsburgh, Pa., *An Evaluation of the Unloading Compliance Procedure for J-Integral Testing in the Hot Cell, Final Report*, NUREG/CR-1070 (ORNL/SUB-7394/1), October 1979.

P. B. Crosley and E. J. Ripling, Materials Research Laboratory, Inc., Glenwood, Ill., *Development of a Standard Test for Measuring KIa with a Modified Compact Specimen*, NUREG/CR-2294 (ORNL/SUB-81/7755/1), August 1981.

H. A. Domian, Babcock and Wilcox Company, Alliance, Ohio, *Vessel V-8 Repair and Preparation of Low Upper-Shelf Weldment*, NUREG/CR-2676 (ORNL/SUB/81-85813/1), June 1982.

R. D. Cheverton, S. K. Iskander, and D. G. Ball, Union Carbide Corp. Nuclear Div., Oak Ridge Natl. Lab., Oak Ridge, Tenn., *PWR Pressure Vessel Integrity During Overcooling Accidents: A Parametric Analysis*, NUREG/CR-2895 (ORNL/TM-7931), February 1983.

J. G. Merkle, Union Carbide Corp. Nuclear Div., Oak Ridge Natl. Lab., Oak Ridge, Tenn., *An Examination of the Size Effects and Data Scatter Observed in Small Specimen Cleavage Fracture Toughness Testing*, NUREG/CR-3672 (ORNL/TM-9088), April 1984.

W. R. Corwin, Martin Marietta Energy Systems, Inc., Oak Ridge Natl. Lab., Oak Ridge, Tenn., *Assessment of Radiation Effects Relating to Reactor Pressure Vessel Cladding*, NUREG/CR-3671 (ORNL-6047), July 1984.

W. R. Corwin, R. G. Berggren, and R. K. Nanstad, Martin Marietta Energy Systems, Inc., Oak Ridge Natl. Lab., Oak Ridge, Tenn., *Charpy Toughness and Tensile Properties of a Neutron Irradiated Stainless Steel Submerged-Arc Weld Cladding Overlay*, NUREG/CR-3927 (ORNL/TM-9709), September 1984.

J. J. McGowan, Martin Marietta Energy Systems, Inc., Oak Ridge Natl. Lab., Oak Ridge, Tenn., *Tensile Properties of Irradiated Nuclear Grade Pressure Vessel Plate and Welds for the Fourth HSST Irradiation Series*, NUREG/CR-3978 (ORNL/TM-9516), January 1985.

J. J. McGowan, Martin Marietta Energy Systems, Inc., Oak Ridge Natl. Lab., Oak Ridge, Tenn., *Tensile Properties of Irradiated Nuclear Grade Pressure Vessel Welds for the Third HSST Irradiation Series*, NUREG/CR-4086 (ORNL/TM-9477), March 1985.

W. R. Corwin, G. C. Robinson, R. K. Nanstad, J. G. Merkle, R. G. Berggren, G. M. Goodwin, R. L. Swain, and T. D. Owings, Martin Marietta Energy Systems, Inc., Oak Ridge Natl. Lab., Oak Ridge, Tenn., *Effects of Stainless Steel Weld Overlay Cladding on the Structural Integrity of Flawed Steel Plates in Bending, Series 1*, NUREG/CR-4015 (ORNL/TM-9390), April 1985.

W. J. Stelzman, R. G. Berggren, and T. N. Jones, Martin Marietta Energy Systems, Inc., Oak Ridge Natl. Lab., Oak Ridge, Tenn., *ORNL Characterization of Heavy-Section Steel Technology Program Plates 01, 02, and 03*, NUREG/CR-4092 (ORNL/TM-9491), April 1985.

G. D. Whitman, Martin Marietta Energy Systems, Inc., Oak Ridge Natl. Lab., Oak Ridge, Tenn., Historical Summary of the Heavy-Section Steel Technology Program and Some Related Activities in Light-Water Reactor Pressure Vessel Safety Research, NUREG/CR-4489 (ORNL-6259), March 1986.

R. H. Bryan, B. R. Bass, S. E. Bolt, J. W. Bryson, J. G. Merkle, R. K. Nanstad, and G. C. Robinson, Martin Marietta Energy Systems, Inc., Oak Ridge Natl. Lab., Oak Ridge, Tenn., *Test of 6-in.-Thick Pressure Vessels. Series 3: Intermediate Test Vessel V-8A - Tearing Behavior of Low Upper-Shelf Material*, NUREG-CR-4760 (ORNL-6187), May 1987.

D. B. Barker, R. Chona, W. L. Fourney, and G. R. Irwin, University of Maryland, College Park, Md., A Report on the Round Robin Program Conducted to Evaluate the Proposed ASTM Standard Test Method for Determining the Plane Strain Crack Arrest Fracture Toughness, K_{Ia}, of Ferritic Materials, NUREG/CR-4966 (ORNL/SUB/79-7778/4), January 1988.

L. F. Miller, C. A. Baldwin, F. W. Stallman, and F. B. K. Kam, Martin Marietta Energy Systems, Inc., Oak Ridge Natl. Lab., Oak Ridge, Tenn., *Neutron Exposure Parameters for the Metallurgical Test Specimens in the Fifth Heavy-Section Steel Technology Irradiation Series Capsules*, NUREG/CR-5019 (ORNL/TM-10582), March 1988.

J. J. McGowan, R. K. Nanstad, and K. R. Thoms, Martin Marietta Energy Systems, Inc., Oak Ridge Natl. Lab., Oak Ridge, Tenn., Characterization of Irradiated Current-Practice Welds and A533 Grade B Class 1 Plate for Nuclear Pressure Vessel Service, NUREG/CR-4880 (ORNL-6484/V1 and V2), July 1988.

R. D. Cheverton, W. E. Pennell, G. C. Robinson, and R. K. Nanstad, Martin Marietta Energy Systems, Inc., Oak Ridge Natl. Lab., Oak Ridge, Tenn., *Impact of Radiation Embrittlement on Integrity of Pressure Vessel Supports for Two PWR Plants*, NUREG/CR-5320 (ORNL/TM-10966), February 1989.

J. G. Merkle, Martin Marietta Energy Systems, Inc., Oak Ridge Natl. Lab., Oak Ridge, Tenn., *An Overview of the Low-Upper-Shelf Toughness Safety Margin Issue*, NUREG/CR-5552 (ORNL/TM-11314), August 1990.

R. D. Cheverton, T. L. Dickson, J. G. Merkle, and R. K. Nanstad, Martin Marietta Energy Systems, Inc., Oak Ridge Natl. Lab., Oak Ridge, Tenn., *Review of Reactor Pressure Vessel Evaluation Report for Yankee Rowe Nuclear Power Station (YAEC No. 1735)*, NUREG/CR-5799 (ORNL/TM-11982), March 1992.

INTERNAL DISTRIBUTION

1–2. C. A. Baldwin
3. B. R. Bass
4. E. E. Bloom
5. T. L. Dickson
6. L. L. Horton
7. D. W. Heatherly
8. S. K. Iskander
9. W. J. McAfee
10. D. E. McCabe
11. J. G. Merkle
12. M. K. Miller
13–20. R. K. Nanstad
21–28. I. Remec
29–36. T. M. Rosseel
37. J. J. Simpson
38–45. M. A. Sokolov
46. R. E. Stoller
47–48. R. L. Swain
49. K. R. Thoms
50. J. A. Wang
51. S. J. Zinkle
52. Office of Technical Information and Classification

EXTERNAL DISTRIBUTION

53. AEA Technology Nuclear Science, Harwell, Didcot, Oxforshire OX1100QJ, United Kingdom

    C. A. English

54. ATI, Inc., Suite 160, 210 Crow Canyon Place, San Ramon, CA 94583

    W. L. Server

55. Babcock and Wilcox, B&W R&D Division, 1562 Beeson St., Alliance, OH 44601

    W. A. Van Der Sluys

56. Bettis Atomic Power Laboratory, Westinghouse Electric Corp., P. O. Box 79 West Mifflin, PA 15122

    M. G. Burke

57. Central Institute for Nuclear Studies, CEN/SCK, Reactor Physics Department, Boeretang 200, B-2400 Mol. Belgium

    E. Van Walle

58. DOE Oak Ridge Operation Office, P. O. Box 2001, Oak Ridge, TN 37831-6269

    S. R. Martin

59. EPRI, 1300 West W.T. Harris Blvd., Charlotte, NC 28262

    S. T. Rosinski

60. Health & Safety Executive, Nuclear Safety Directorate, HM Nuclear Installation Inspectorate, St. Peter's House, Stanley Precinct, Bootle, Merseyside L203LZ, United Kingdom

    R. D. Nicholson

61. Joint Research Center, Institute for Advanced Materials, P. O. Box 2 Petten, 1775 Petten, The Netherlands

    L. Debarberis

62. Korea Atomic Energy Research Institute, Nuclear Material Technology Division, 150 Dukjin-dong, Yusong-ku, 305-353 Daejon, Korea

    Dr. Bong Sang Lee

63. Nuclear Electric plc, Berkeley Technology Centre, Berkeley, Gloucestershire, GL 13 9PB, United Kingdom

    C. J. Bolton

64. Nuclear Research Institute, Division of Nuclear Materials, 250 68 REZ, Czech Republic

    M. Brumovsky

65–71. NRC, RES/DET, Washington, DC, 20555-0001

R. J. Barrett	C. J. Fairbanks
A. L. Hiser	M. T. Kirk
S. M. Malik	J. L. Uhle
M. E. Mayfield	

72–73. NRC, NRR/DE, Washington, DC, 20555-0001

    B. J. Elliot
    M. A. Mitchell

74. Pavinich, W. A., 1113 Laurel Hill Road, Knoxville, TN 37923

75–76. Prometey, Central Research, Institute of Structural Materials, 193167 Sankt Petersburg, Russia

    V. A. Nikolaev
    B. Z. Margolin

77. Rolls-Royce and Associates LTD., P. O. Box 31, Raynesway, Derby DE24 8BJ, United Kingdom

T. J. Williams

78. Paul Scherrer Institute, CH-5233 VILLIGEN SPI, Switzerland

D. Kalkhof

79. Siemens AG, KWU S514, Freyeslebenstrasse 1, D-8520 Erlangen, Germany

R. Langer

80–82. Staatliche Materialprufungsanstalt and Der Universitat Stuttgart, Pfaffenwaldring 32, 7 Stuttgard 80, Germany

J. Fohl
E. Roos
U. Eisele

83–84. Tokai Research Establishment, Japan Atomic Energy Research Institute, 2-4 Shirakata-shirane, Tokai-mura, Naka-gun, Ibaraki 319-1195, Japan

M. Suzuki
K. Onizawa

85. Tokai University, Dept. of Nuclear Engineering, 1117, Kitakaname, Hiratsuka-shi, Kanagawa-Ken 259-12, Japan

Prof. Shiori Ishino

86–88. University of California, Department of Chemical and Nuclear Engineering, Ward Memorial Drive, Santa Barbara, CA 93106

D. Klingensmith
G. E. Lucas
G. R. Odette

89–91. University of Michigan, Ford Nuclear Reactor, 2301 Bonisteel Blvd., Ann Arbor, MI 48109-2100

C. W. Becker
D. Wehe
P. A. Simpson

92. University of Missouri-Rolla, Department of Nuclear Engineering, Rolla, MO 65401

A. S. Kumar

93. University of Tennessee, Mechanical Aerospace & Biomedical Engineering, 314 Perkins Hall, 1506 Middle Drive, Knoxville, TN 37996

    J. D. Landes

94. U.S. Department of Energy, Office of Nuclear Science and Technology, 19901 Germantown Rd., Germantown, MD 20874-1290

    R. M. Versluis

95. VTT Manufacturing Technology, P. O. Box 1704, FIN-02044 VTT, Finland

    K. Wallin
    M. Valo

96. Westinghouse, P. O. Box, 500, Mail Code 9483-1903, Windsor, CT 60695

    S. T. Byrne

97. Westinghouse Electric Corporation, P. O. Box 335, Pittsburgh, PA 15230

    W. Bamford

98. Westinghouse R&D Center, 1310 Beulah Rd., Pittsburgh, PA 15325

    R. G. Lott

NRC FORM **335**
(2-89)
NRCM 1102,
3201, 3202

U.S. NUCLEAR REGULATORY COMMISSION

BIBLIOGRAPHIC DATA SHEET

(See instructions on the reverse)

1. REPORT NUMBER
(Assigned by NRC, Add Vol., Supp., Rev., and Addendum Numbers, if any.)

NUREG/CR-
ORNL/TM-2002/293

2. TITLE AND SUBTITLE

Fracture Toughness of an Irradiated, Highly Embrittled Reactor Pressure Vessel Weld

3. DATE REPORT PUBLISHED

MONTH	YEAR

4. FIN OR GRANT NUMBER

W6953

5. AUTHOR(S)

M. A. Sokolov, R. K. Nanstad, I. Remec, C. A. Baldwin, and R. L. Swain

6. TYPE OF REPORT

Technical

7. PERIOD COVERED *(Inclusive Dates)*

8. PERFORMING ORGANIZATION - NAME AND ADDRESS *(If NRC, provide Division, Office or Region, U.S. Nuclear Regulatory Commission, and mailing address; if contractor, provide name and mailing address.)*

Oak Ridge National Laboratory
Oak Ridge, TN 37831-6151

9. SPONSORING ORGANIZATION - NAME AND ADDRESS *(If NRC, type "Same as above"; if contractor, provide NRC Division, Office or Region, U.S. Nuclear Regulatory Commission, and mailing address.)*

Division of Engineering Technology
Office of Nuclear Regulatory Research
U.S. Nuclear Regulatory Commission
Washington, DC 20555-0001

10. SUPPLEMENTARY NOTES

C. J. Fairbanks, NRC Program Manager

11. ABSTRACT *(200 words or less)*

A radiation-sensitive reactor pressure vessel weld with intentionally enhanced copper content, designated KS-01, is characterized by its static initiation (KIc, KJc) and Charpy impact toughness in the unirradiated and irradiated conditions. The objective of this Heavy-Section Steel Irradiation (HSSI) Program project is to investigate the ability of highly embrittled material to maintain the shape of the unirradiated transition fracture toughness curve, as well as to examine the ability of the Charpy 41-J shift to predict the fracture toughness shift at high levels of embrittlement. Irradiations were performed at the University of Michigan Ford Nuclear Reactor in the HSSI IAR facility. Specimens of KS-01 weld were irradiated up to about 0.74 x 1019 n/cm2 at 288 oC resulting in a ductile to brittle transition-temperature shift of 169 oC. It was anticipated that this shift would result in a fracture toughness transition temperature (at 100 MPa÷m) in the irradiated condition near or slightly above the pressurized thermal-shock screening criterion for weld metals, of 300oF (149oC) according to the Code of Federal Regulations, Title 10, Part 50 (10CFR50). The fracture toughness characterization of the unirradiated and irradiated KS-01 weld was mainly performed by testing 1T C(T) although 0.5T C(T) and precracked Charpy specimens were also used.

12. KEY WORDS/DESCRIPTORS *(List words or phrases that will assist researchers in locating the report.)*

Reactor Pressure Vessel
Fracture Toughness
Weld
Highly Embrittled
Irradiation
PTS
C(T) Specimens
Charpy Impact

13. AVAILABILITY STATEMENT

Unlimited

14. SECURITY CLASSIFICATION

(This Page)
Unclassified

(This Report)
Unclassified

15. NUMBER OF PAGES

16. PRICE

This form was electronically produced by Elite Federal Forms, Inc.